

Design and Development of Tetrahydro-Quinoline Derivatives as Dual mTOR-C1/C2 Inhibitors for the Treatment of Lung Cancer

Udit J. Chaube, Rakesh Rawal, Abhishek B. Jha, Bhavesh Variya, Hardik G. Bhatt

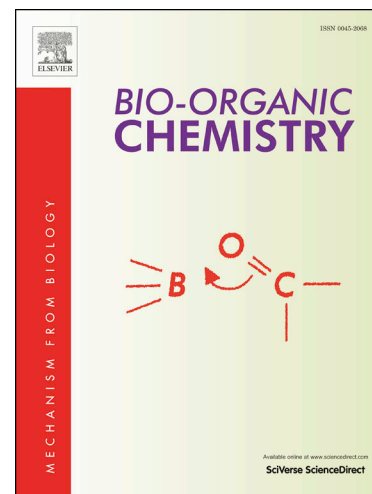
PII: S0045-2068(20)31799-5
DOI: <https://doi.org/10.1016/j.bioorg.2020.104501>
Reference: YBIOO 104501

To appear in: *Bioorganic Chemistry*

Received Date: 22 August 2020
Revised Date: 8 October 2020
Accepted Date: 20 November 2020

Please cite this article as: U.J. Chaube, R. Rawal, A.B. Jha, B. Variya, H.G. Bhatt, Design and Development of Tetrahydro-Quinoline Derivatives as Dual mTOR-C1/C2 Inhibitors for the Treatment of Lung Cancer, *Bioorganic Chemistry* (2020), doi: <https://doi.org/10.1016/j.bioorg.2020.104501>

This is a PDF file of an article that has undergone enhancements after acceptance, such as the addition of a cover page and metadata, and formatting for readability, but it is not yet the definitive version of record. This version will undergo additional copyediting, typesetting and review before it is published in its final form, but we are providing this version to give early visibility of the article. Please note that, during the production process, errors may be discovered which could affect the content, and all legal disclaimers that apply to the journal pertain.



Design and Development of Tetrahydro-Quinoline Derivatives as Dual mTOR-C1/C2 Inhibitors for the Treatment of Lung Cancer

Udit J. Chaube¹, Rakesh Rawal², Abhishek B. Jha³, Bhavesh Variya³, Hardik G. Bhatt^{1*}

¹ Department of Pharmaceutical Chemistry, Institute of Pharmacy, Nirma University, Ahmedabad 382 481. India.

² Department of Life Sciences, Gujarat University, Ahmedabad 380 009. India.

³ Department of Pharmacology, Institute of Pharmacy, Nirma University, Ahmedabad 382 481. India.

*Address for correspondence: Department of Pharmaceutical Chemistry, Institute of Pharmacy, Nirma University, S.G. Highway, Chharodi, Ahmedabad 382 481. India.

Phone no. +91 79 71652727; Fax no. +91 2717 241916; Email Id: hardikbhatt23@hotmail.com

Abstract

Lung cancer is one of the most prevailed cancer worldwide. Many genes get mutated in lung cancer but the involvement of EGFR, KRAS, PTEN and PIK3CA are more common. Unavailability of potent drugs and resistance to the available drugs are major concern in the treatment of lung cancer. In the present research, mTOR was selected as an important alternative target for the treatment of lung cancer which involves the PI3K/AKT/mTOR pathway. We studied binding interactions of AZD-2014 with the mTOR protein to identify important interactions required to design potent mTOR inhibitors which was supported by QSAR studies. Pharmacophore based virtual screening studies provided core scaffold, THQ. Based on molecular docking interactions, 31 THQ derivatives were synthesized and characterized. All compounds were screened for cellular mTOR enzyme assay along with antiproliferative activity against the panel of cancerous cell lines, from which 6 compounds were further screened for colony forming assay. Two most potent compounds, HB-UC-1 and HB-UC-5, were further screened for flow cytometry analysis, gene expression study and western blot analysis. Gene expression study revealed the efficiency of compound HB-UC-1 against both mTORC1 and mTORC2 by affecting downstream regulators of mTORC1 (E_4BP_4 , eIF_4EBP_1) and mTORC2 (PCK1), respectively. In western blot analysis, both compounds, inhibited phosphorylation of AKT S473 which proved the efficiency these compounds against the mTORC2. These two compounds were further screened for *in-vivo* biological evaluation. Both compounds increased lifespan of cancer-bearing animals with improvement in mean survival time. Further, in bezopyrene induced lung cancer animal model, both compounds showed effectiveness through the biochemical parameters and histopathological evaluation of the lung tissue. In future, potent hit compound from this series could be modified to develop lead mTOR inhibitors for the treatment of lung cancer.

Keywords: mTOR, Lung Cancer, Pharmacophore, QSAR, X-ray Crystallography, Tetrahydroquinoline

Introduction

Recent cancer statistics reveal that the lung cancer is one of the most prevailed cancer worldwide. It is mainly classified as small cell lung cancer (SCLC) and non-small cell lung cancer (NSCLC); among which, cases of NSCLC (85%) are more as compared to SCLC. [1] NSCLC is further classified as adenocarcinoma (AC), squamous cell carcinoma (SCC), and large cell carcinoma (LCC). Many genetic mutations take place in lung cancer, but KRAS, EGFR, PIK3CA and PTEN are most common. [2-4] KRAS and EGFR mutations are found in AC, [1,3] while PIK3CA and PTEN mutations occur in the case of SCC. [5] No drugs are available in the market which directly acts on KRAS [1] and this problem can be solved by targeting the pathway associated with KRAS mutant in NSCLC viz. RAS/RAF/MEK or PI3K/AKT/mTOR pathway. Selumetinib and BEZ-235 are available in the market for targeting the RAS/RAF/MEK and PI3K/AKT/mTOR pathway, respectively. Similarly in the case of EGFR-mutant AC, drugs available in market are Gefitinib and Erlotinib. [3] Major problem associated with these drugs is resistance [4,5] which results into decrease in therapeutic efficacy. As per the available literature, it is well understood that PI3K/AKT/mTOR pathway is altered in lung cancer [6] and discovery of new inhibitors against any target of this pathway could be helpful for the treatment of lung cancer. Hence in the present research work, mTOR was selected as the choice of target as it is downstream to PI3K/AKT and its inhibition may completely block the pathway.

mTOR (Mammalian/Mechanistic Target of Rapamycin) consists of two subunits viz. mTORC1 (mTOR Complex-1) and mTORC2 (mTOR Complex- 2) among which mTORC-1 is considered as rapamycin sensitive target while on the other hand, mTORC2 is considered as rapamycin insensitive target. [7,8] Most of the rapalogues (Rapamycin analogue) act on mTORC-1 via FKBP12 and allosterically inhibit its activity [9-11] while on the other side, these compounds are unable to inhibit the mTORC-2. mTORC-1 consists of Raptor, Deptor, mLST8, and PRAS-40. [12] Excessive mTORC-1 activity results into the phosphorylation of the S6K which is downstream to the mTORC-1 and results into the uncontrolled protein synthesis, cell proliferation and angiogenesis. Similarly, eIF4EBP1 is also present in downstream to the mTORC1, where mTORC-1 acts as negative regulator of eIF4EBP1, resulting into decrease level of eIF4EBP1 which further results in increase level of protein synthesis and uncontrolled cell proliferation [6]. While on the other side, mTORC-2 consists of Rictor-mSin-1 complex instead of Raptor which is the only difference between the mTORC-1 and

mTORC-2.^[12] This Rictor-mSin-1 complex generates steric hindrance to the Rapamycin-FKBP12 complex which results into the insensitivity of mTORC-2 protein toward the rapamycin and rapalogues.^[13] In the present research work, efforts were made to design and synthesize small molecules which inhibit both, mTORC-1 and mTORC-2 to avoid problems arises due to resistance and could be further explored in the treatment of lung cancer.

Results and Discussion

Design of Compounds

As per the available literature, it is well understood that PI3K/AKT/mTOR pathway is altered in lung cancer and discovery of new inhibitors against any target on this pathway might be helpful for the treatment of lung cancer. Therefore in the present research work, efforts were made to discover novel compounds that inhibited mTOR and could be used to treat lung cancer. Effectiveness of designed compound depends upon how precisely it binds with important amino acids of target receptor and orient itself in binding pocket, so to inhibit target protein. To start with design of novel inhibitors, we studied binding pocket of mTOR and also performed conventional ligand based and structure based computational approaches.

Binding pocket of mTOR (PDB ID:4JT6) in complex with the PI-103 (as shown in Figure 1(A)) consisted of many important amino acids which included hydrophobic amino acids viz. Leu2185, Ile2237, Val2240, Ile2356; polar amino acid Tyr2225 and charged amino acid Asp2357. Among all these amino acids, Asp2195 and Tyr2225 were present in inner binding pocket and formed two hydrogen bonds with the phenolic group of co-crystallized ligand PI-103, while Val2240 of hinge region was one of the crucial amino acid responsible for high affinity of compound PI-103 with the mTOR protein. As our research is mainly focused on the lung cancer therapy via mTOR inhibition; hence, AZD-2014 was selected to study in detail for the designing process as currently, it is in clinical trial for the treatment of lung cancer (as mTOR inhibitor). The binding mode of AZD-2014 with mTOR protein depicted in Figure 1(B). The

AZD-2014 was discovered by modifications from AZD-8055 (as shown in Figure 1(C)). This modification was carried out to reduce its residence time in the hepatocyte which may improve the pharmacokinetics and lower the risk of liver toxicity. For the accomplishment of this objective, benzyl alcohol of AZD-8055 was replaced by benzyl amide which dramatically improved aqueous solubility, but resulted into slight decline in the potency. One of the reason of the reduction in the potency of the compound AZD-2014 was its inability to form hydrogen bonds with the Tyr2225 and Asp2195 as depicted in Figure 1(B) which is seen in the case of standard co-crystallized ligand PI-103. Oxygen of the morpholine ring substituted on the AZD-2014 formed the hydrogen bond with the hinge region (Val2240) of the mTOR protein and potentially inhibited both mTORC1 and mTORC2. It also showed selectivity against the mTOR as compared to the other isoforms of PI3K. The detailed literature review of AZD-2014 revealed that the amide group is responsible for the solubility and less residence time of this compound in the hepatocyte. Detailed study of target protein provided deep insight about important interactions and their effects on activity.

Detailed study on binding mode of compounds PI-103 and AZD-8055 with the mTOR protein concluded that interactions with specific amino acids like Tyr2225, Asp2195 and Val2240 are essential to produce potent inhibitory effect. Apart from this, in compound AZD-2014, amide linkage played an important role for the improvement of the solubility and reduction in the liver toxicity. Hence, according to this fact, two amide groups were kept at R₁ and R₂ in design of proposed derivatives as depicted in the Figure 1(C). Additionally, it was also observed that the oxygen of the morpholine ring substituted on the AZD-2014 was essential for the binding interaction with the hinge region (Val2240) of the mTOR protein. Thus, in many of final derivatives, halogen substitutions were introduced which revealed similar binding interactions with hinge region (Val2240) of the mTOR protein.

To validate the hypothesis of design of molecules based upon AZD-2014 for the identification of the functional groups required for the mTOR inhibition, 3D-QSAR studies (CoMFA and CoMSIA) were performed on 50 pyridoaminotropanes/tetrahydroquinazoline derivatives and 28 benzoxazepine derivatives which are already reported as mTOR inhibitors. The results are already published,^[14,15] but for better understanding of designed molecules, brief about both studies are provided. In case of pyridoaminotropanes/tetrahydroquinazoline derivatives, three diverse alignment methods viz. docking based, distil based &

pharmacophore based alignments were used with distill method was found to be the best method as it gave the good statistical results in the form of leave-one-out cross-validated coefficients (q^2), conventional coefficient (r^2) and predicted correlation coefficient (r^2_{pred}). In case of CoMFA, q^2 , r^2 and r^2_{pred} were found to be 0.664, 0.992, and 0.652, respectively. While in case of CoMSIA, 25 different models were produced among which the amalgamation of steric, electrostatic & hydrophobic i.e. SEH and steric, electrostatic, hydrophobic, donor & acceptor, i.e. SEHDA were found as best amalgamation. In case of CoMSIA (SEH) the statistical values in terms of q^2 , r^2 and r^2_{pred} were found to be 0.664, 0.992, and 0.652, respectively. Similarly, in case of CoMSIA (SEHDA) the values of q^2 , r^2 and r^2_{pred} were found to be 0.739, 0.976, and 0.779, respectively. Furthermore, with the aid of these CoMFA and CoMSIA models various contour maps were generated. These generated contour maps were validated by the molecular docking study. Based upon the analysis of contour maps, important features of pyridoaminotropanes/tetrahydroquinazoline were identified which were responsible for the mTOR inhibition. This included substitutions favorable with bulky groups, electropositive/electronegative groups, proton donor atoms and hydrophilic groups. Similar to the earlier study, 28 benzoxazepine derivatives were also explored for the CoMFA and CoMSIA analysis. Here also distil alignment was found to be the best alignment among all these three alignments as it provided good statistical results in the form of Leave One Out (LOO), cross validated coefficients (q^2), conventional coefficient (r^2) and predicted correlation coefficient (r^2_{pred}). In case of CoMFA; q^2 , r^2 and r^2_{pred} values were found to be 0.615, 0.990 and 0.930, respectively. While in the case of CoMSIA; q^2 , r^2 and r^2_{pred} values were found to be 0.748, 0.986 and 0.933, respectively. Furthermore, generated contour maps were validated by the molecular docking study where specific positions of benzoxazepine scaffold was found to be favorable for bulky groups, for hydrogen bond acceptor groups, for electron donating groups, hydrogen bond acceptor atom, and hydrophobic functional groups. Overall, with the aid of this 3D-QSAR studies, important structural features required for the mTOR inhibition were identified and incorporated in designed of our tetrahydroquinoline derivatives.

The study gave the critical insights of functional groups required for the mTOR inhibition as depicted in Figure 1(D). Outcome of 3D-QSAR study proved presence of substitutions along with importance of amide substitution for the mTOR inhibition. In this 3D-QSAR studies, distil alignment was found to be the best alignment method as it gave good statistical results with good contour maps orientations.

Contours maps validated by molecular docking study revealed that R₁ position of tetrahydroquinoline substituted with the hydrogen bond acceptor atom, polar functional groups, or combinations of electropositive or electronegative groups might be useful for the mTOR inhibition. Similarly, R₂ position of tetrahydroquinoline substituted with the bulky functional group, hydrogen bond acceptor atom, and hydrophobic functional groups might be useful for the mTOR inhibition. Thus, with the combination of ligand based approaches like CoMFA and CoMSIA and structure based approach like molecular dynamics and simulations assisted molecular docking study, important features required for mTOR inhibition were identified and incorporated in the THQ scaffold, finalized from pharmacophore based virtual screening method.

Simultaneously, pharmacophore modelling followed by virtual screening were used for identification of core scaffold. six potent mTOR inhibitors viz. Torin-1, Torin-2, AZD-2014, WYE-354, WYE-687, and WAY-600 reported as mTOR inhibitors (shown in supporting information material as Figure SF-1) were selected from the literature. Selection criteria was mainly emphasized on the in-vitro potency and pharmacokinetic profile of the compounds. With the help of these six mTOR inhibitors; total four pharmacophore models were generated (shown in supporting information material as Table ST-1) in which model_1 with highest D_{MEAN} score was selected and all six drug like molecules contributed for its generation. The best pharmacophore model contained 4 features viz. two hydrophobic features (HY_1 and HY_2), one acceptor atom (AA_1) and one acceptor site (AS_1) of the receptor protein inhibitors (shown in supporting information material as Figure SF-2). This model was further validated with two well-known statistical methods viz. Receiver Operating Characteristics (ROC) (shown in supporting information material as Figure SF-3) and Gunner Henry (GH) scoring methods (shown in supporting information material as Table ST-2). The best and validated pharmacophore model was used for virtual screening process thorough NCI database. Virtual screening provided thousands of compounds and after necessary filtering, it was concluded that compounds with THQ as a core scaffold showed best results. (Details of pharmacophore based virtual screening are provided in supporting information file).

Overall in the design process of the novel compounds; pharmacophore based virtual screening ^[16] was carried out for the identification of the core scaffold while knowledge based drug design approach to study target protein and 3D-QSAR studies ^[17] were carried out for

the identification of the substituents required for mTOR inhibition. With the aid of these approach, several hundreds of tetrahydroquinoline (THQ) derivatives were designed. Further, these designed THQ derivatives were filtered through the molecular dynamics assisted molecular docking study which resulted into 31 THQ derivatives showing comparable docking score as that of the co-crystallized ligand (PI-103) of mTOR protein along with good binding affinity. As per the molecular docking study, compound HB-UC-1 was found to be most effective mTOR inhibitor as it showed all necessary interactions with the mTOR protein as shown in supporting information.

Docking of Designed Compounds

Tetrahydroquinoline was selected as core scaffold based upon the pharmacophore based virtual screening and *in-silico* ADMET studies (shown in supporting information material as Table ST-3 and ST-4 and additional details of selection of core scaffold is given in the supporting information material). Initially tetrahydroquinoline as core scaffold showed very less docking score compared to the standard PI-103 (shown in supporting information material as Table ST-4). Although, incorporation of the required substituents, on the basis of study of target receptor and QSAR study, to the tetrahydroquinoline scaffold drastically increased the docking score of designed compounds which was comparable with the standard co-crystallized ligand, PI-103 (showed in supporting information material as Table ST-5). All designed compounds were docked ^[18-20] on the mTOR protein (4JT6) to select few which formed important interactions with target protein and could be proved as potent mTOR inhibitor. Compounds HB-UC-1, HB-UC-3 and HB-UC-11 from series-I showed good docking score with protein as (depicted in supporting information material as Table ST-5). Similarly in the case of series-II, compounds HB-UC-15, HB-UC-17 and HB-UC-21 showed good docking score. Likewise in series III, docking results revealed that the compounds HB-UC-31, HB-UC-33 and HB-UC-37 were topmost compounds in terms of the docking score. Overall, compound HB-UC-1 was found to best compounds as it showed all important binding interactions with the crucial amino acid including Val2240 which is present in hinge region of the mTOR protein. Additionally, compound HB-UC-1 showed binding interaction with the Asp2195 and Tyr2225 which is similar to the binding interactions of compound PI-103 with the mTOR protein (shown in supporting information material as Figure SF-4A and 4B). One important observation was revealed in this docking study that these topmost molecules; HB-

UC-1, HB-UC-3, HB-UC-15, HB-UC-17, HB-UC-31, HB-UC-33 consisted of electron withdrawing groups at R₁ and R₂ position of THQ ring which clearly indicated that these electron withdrawing groups are playing important role in the binding with the mTOR protein.

***In-Silico* ADMET and Toxicity Prediction**

OSIRIS property explorer is generally used for the prediction of toxicity in the form of mutagenic, tumorigenic, irritant and reproductive effect. Additionally, it also provides the information about the physicochemical properties of designed molecules in the form of clogP (log C octanol/log C water), TPSA (The Polar Surface Area), solubility, molecular weight, drug score and drug likeness. admetSAR is also widely used for the prediction of Adsorption, Distribution, Metabolism and Excretion along with the acute oral toxicity in the form of class-I chemicals ($LD_{50} \leq 50\text{mg/kg}$), class-II chemicals ($500\text{mg/kg} > LD_{50} > 50\text{mg/kg}$), class-III chemicals ($5000\text{mg/kg} > LD_{50} > 500\text{mg/kg}$) and class-IV chemicals ($LD_{50} > 5000\text{mg/kg}$). It also gives an idea about the carcinogenicity of the chemical. In the present study, both the online tools were used for ADMET property determination. Top 31 newly designed THQ derivatives were further used for the ADMET prediction with the help of OSIRIS Property Explorer and admetSAR. Most of the marketed drugs having aqueous solubility in between -6 to 0. Hence the compounds which showed aqueous solubility in between these value considered as a good candidate for absorption and distribution. Among these 31 designed compounds, Series-III compounds revealed good aqueous solubility as compared to series-I and series-II compounds. While in case of series-I and series-II the aqueous solubility was acceptable as most of the compounds shown solubility around -6. In case of TPSA, most of the designed molecules were far away from the TPSA value of standard drug AZD-8055. Although some of the designed compounds HB-UC-1, HB-UC-15 and HB-UC-31 showed TPSA value close to AZD-8055. Among the 31 designed compounds, most of the compounds from all three series showed a clogP value less than 5 (data are provided in supporting information material tables ST-6A, ST-6B and ST-6C). From series-I, compounds like HB-UC-1, HB-UC-5, HB-UC-6, HB-UC-11, HB-UC-13 and HB-UC-14 showed clogP less than 5 indicating that they might get absorbed properly as shown in supporting information material table ST-6A. Similarly, from series-II compounds, HB-UC-15, HB-UC-18, HB-UC-19, HB-UC-20, HB-UC-24 and HB-UC-25 showed clogP values less than 5 (data are provided in supporting information material table ST-6B).

From series-III compounds, HB-UC-31, HB-UC-34, HB-UC-36, HB-UC-39 and HB-UC-41 showed clogP values less than 5 (as shown in supporting information material table ST-6C). In addition to that, maximum number of designed compounds were found to be non-mutagenic, non-tumorigenic, non-irritant and no bad effects on reproductive system except compounds of series-III (shown in supporting information material table ST-6C). All newly designed compounds of series-III revealed irritant effect (shown in supporting information material table ST-6C). In addition to that, compounds from series I and II indicated some toxic effect viz. HB-UC-14, HB-UC-19 and HB-UC-25. Similarly in the case of admetSAR, most of the compounds from all the series showed Human Intestinal Absorption (HIA) along with the Blood Brain Barrier (BBB) absorption (shown in supporting information material table ST-7). Some of the designed compounds showed Caco-2 permeability indicated that these compounds may get orally absorbed in the intestine. All designed compounds were found to be non-carcinogen and showed distribution in the mitochondria and fell in the category of class-III chemicals ($500\text{mg/kg} > \text{LD}_{50} < 5000\text{mg/kg}$) (shown in supporting information material table ST-7) except compound HB-UC-14 which fell in the category of class-II chemical ($500\text{mg/kg} > \text{LD}_{50} > 50\text{mg/kg}$).

Chemistry

Based upon the ligand based and structure based approach, 31 tetrahydroquinoline (THQ) derivatives were designed and synthesized with the help of suitable synthetic scheme as depicted in Figure 2.

THQ was treated with the 9-fluorenylmethoxycarbonyl (Fmoc) for the protection at nitrogen of THQ which resulted into selective nitration at 6th position of the THQ when treated with potassium nitrate and sulfuric acid. Normally during this nitration reaction, electrophile attack of nitro group could take place at 6th and 8th of THQ. Due to protection with Fmoc, electrophilic attack at 8th position of THQ get hindered and thus selective nitration was occurred at 6th position of THQ.^[21] After the nitration of Fmoc protected THQ, it was reacted with pyrrolidine for the deprotection followed by the reaction with three different acid chlorides viz. 4-chlorobenzoyl chloride, benzoyl chloride and 2-ethylbutanoyl chloride showed as R₁ in the synthetic scheme. Further, this compound is treated with the ammonium

chloride and zinc which resulted into the reduction of nitro group into amine. This primary amine was reacted with the different acid chlorides and sulfonyl chlorides (showed as R₂) which resulted into the synthesis of 31 novel desired THQ derivatives. Further, all synthesized derivatives were characterized by ¹H & ¹³C NMR, Mass analysis, and FTIR while the purity was checked by HPLC. In addition to this, structural confirmation was carried out with the help of XRD analysis. Compound HB-UC-25 was taken as the representative compound for the single crystal development and XRD analysis proved synthesis of desired compound.

The chemical structures of all compounds were confirmed by FTIR, ¹H & ¹³C NMR and mass spectral analysis. Single crystal XRD finally proved confirmation of series. The purity of the compounds were determined from HPLC analysis and all compounds are having >95% purity. All intermediates along with the final 31 derivatives showed molecular ion peak in mass spectra along with typical halogen pattern in few. Additionally, all intermediates along with the final derivatives were confirmed with FTIR. All final derivatives showed single peak of secondary amine (-NH) at 3300-3390 cm⁻¹ along with the carbonyl groups (-C=O) at 1500-1650 cm⁻¹ which confirmed the formation of the amide bond. Likewise, ¹H NMR showed D₂O exchangeable amide bond proton (-NHCO-) peak around 9-11 ppm (δ value). ¹H NMR also revealed that the signals in between 1 to 4 ppm (δ value) corresponded to the hydrogen attached to the aliphatic carbons of the THQ. Additionally, some aliphatic side chain compounds like HB-UC-6, HB-UC-14, HB-UC-20, HB-UC-36, and HB-UC-41 showed peaks of proton in same region of THQ, i.e. 1 to 4 ppm (δ value). ¹³C NMR analysis was carried out to confirm the number of carbon atoms of the THQ derivatives. The peaks around 160-178 ppm (δ value) of ¹³C NMR indicated the number of carbonyl carbons. Peaks in between 20-60 ppm (δ value) indicated presence of aliphatic carbons of THQ. In addition to this, aliphatic side chains were present in some compounds as mentioned earlier which indicated the peaks in the same aliphatic region of THQ viz. 20-60 ppm (δ value) (Various spectra and HPLC data of final THQ derivatives are given in the supporting information material). The final structural confirmation was carried out by XRD analysis. Compound HB-UC-25 was used as a representative compound for the single crystal development and for XRD analysis, which gave the exact synthesized structure of the desired compound HB-UC-25 with CCDC number 1874590 (Details are given in supporting information material as Figure SF-5 and Table ST-6).

mTOR Enzyme Assay and Structure Activity Relationship Study

All synthesized compounds were evaluated for *in-vitro* mTOR enzyme assay ^[22,23] to prove their potency. Measurement of cellular level of mTOR in A549 cell line indicated that the maximum number of compounds of series-I were found to be potent (as shown in Table 1). In case of series-I compounds, HB-UC-1 ($IC_{50} = 3.17 \pm 0.19 \mu M$) and HB-UC-5 ($IC_{50} = 3.42 \pm 0.34 \mu M$) were found to be most potent among all the other compounds of series-I. The mTOR inhibitory activity of these compounds were found close to the standard AZD-8055 ($IC_{50} = 1.5 \pm 0.31 \mu M$) which is dual mTORC1 and mTORC2 inhibitor. While on the other hand, HB-UC-1 and HB-UC-5 were found to be more potent than standard mTORC1 inhibitor viz. Everolimus ($IC_{50} = 7.5 \mu M$) revealing the importance of the small molecule dual mTORC1 and mTORC2 inhibitor.

In case of mTOR enzyme assay, the study proved the importance of the balanced polarity and hydrophobicity at R_1 position of THQ. As soon as the chlorobenzene group at R_1 was replaced by a simple benzene ring, it resulted in a drastic reduction in the potency of the compounds. This proved that chloro substitution on phenyl ring at R_1 position imparted polarity to the compound and is important for activity. Similarly, aliphatic side chain in series-III at R_1 was not found to be effective for the mTOR inhibition. These results validated the outcome of 3D-QSAR where our hypothesis indicated the importance of the polar functional group, hydrophobicity and hydrogen bond acceptor for the mTOR inhibition. Though there was a hydrophobic group at R_1 in series-II and series-III, a reduction in the polarity was observed due to the absence of chloro substitution on the ring or aliphatic side chain. In the case of the series-I, the polar functional groups along with the hydrophobic groups at R_2 position played an important role. Compounds HB-UC-1 ($IC_{50} = 3.17 \pm 0.19 \mu M$) and HB-UC-5 ($IC_{50} = 3.42 \pm 0.34 \mu M$) were found as most potent among all the compounds of series-I and they explained the importance of polarity due to the nitro and amino group at this position. In addition to this, R_2 position of compounds HB-UC-1 and HB-UC-5 consisted of the phenyl ring in the form of aminophenyl and nitrophenyl rings, respectively, which imparted proper hydrophobic and hydrophilic balance which is also required for the activity.

This hypothesis also proved right in case of the compounds HB-UC-4 ($IC_{50} = 13.09 \pm 0.23 \mu M$) and HB-UC-7 ($IC_{50} = 15.75 \pm 0.51 \mu M$) where hydrogen and methyl groups were presented on benzoyl group at R_2 position, respectively, which resulted in the decrease in the activity of these compounds.

Interestingly, it came to our notice that in the compounds HB-UC-9 ($IC_{50} = 18.24 \pm 0.45 \mu M$) and HB-UC-10 ($IC_{50} = 14.74 \pm 0.38 \mu M$), the increased in bulkiness at R_2 position above the optimum level decreased the activity. This outcome proves that the only increase in the bulkiness or polarity alone will not increase the activity. Proper balance of the hydrophobicity and hydrophilicity is required. The bulkier groups are required at R_2 position with appropriate polarity, but in case it goes beyond the optimum level, the activity decreases. This hypothesis is proved by the compounds HB-UC-2, HB-UC-3 & HB-UC-10. In case of these compounds, the order of potency was found to be HB-UC-3 ($IC_{50} = 4.77 \pm 0.18 \mu M$) > HB-UC-2 ($IC_{50} = 11.06 \pm 0.34 \mu M$) > HB-UC-10 ($IC_{50} = 14.74 \pm 0.38 \mu M$). This difference was observed due to the presence of different halogens at R_2 position. In case of compound HB-UC-3, bromine is present at the R_2 position in the form of bromophenyl which is optimum for balancing the hydrophobic and polar property. As soon as the polarity at R_2 position increases above the optimum level, the activity decreases as it was observed in case of compounds HB-UC-2 and HB-UC-10 where chlorophenyl and fluorenyl were present, respectively.

During the designing part, bioisosteric replacement of a carbonyl group ($C=O$) was carried out by the sulfonyl group ($O=S=O$) which again resulted in decreased activity. This was validated by the compounds HB-UC-2 ($IC_{50} = 11.06 \pm 0.34 \mu M$) and HB-UC-13 ($IC_{50} > 25 \mu M$) where compound HB-UC-2 consisted of a carbonyl group ($C=O$) while HB-UC-13 consisted of sulfonyl group ($O=S=O$) at R_2 position.

***In-Vitro* Antiproliferative MTT Assay and Structure Activity Relationship Study**

All synthesized compounds were screened against panel of four proliferative cell lines by MTT assay ^[24,25] along with four standards; Everolimus, Cisplatin, AZD-8055 and PI-103 as shown in Table 1. Among all synthesized compounds, most of the compounds were found to be potent against these panel of cancer cell lines. In case of Lung Cancer (A549) cell line, the maximum number of compounds were found to be effective. Compounds like HB-UC-1 ($IC_{50} = 0.06 \pm 0.27 \mu M$), HB-UC-3 ($IC_{50} = 0.657 \pm 0.39 \mu M$), HB-UC-5 ($IC_{50} = 0.224 \pm 0.45 \mu M$) and HB-UC-6 ($IC_{50} = 0.158 \pm 0.38 \mu M$) were found to be most potent compounds among all the synthesized compounds. The compound HB-UC-1 was found several fold more potent than the standard compounds viz. Everolimus ($IC_{50} = 6.09 \pm 0.21 \mu M$),

Cisplatin ($IC_{50} = 3.15 \pm 0.19 \mu M$), AZD-8055 ($IC_{50} = 8.17 \pm 0.25 \mu M$) and PI-103 ($IC_{50} = 1.65 \pm 0.34 \mu M$); while compounds HB-UC-3 ($IC_{50} = 0.657 \pm 0.39 \mu M$), HB-UC-5 ($IC_{50} = 0.224 \pm 0.45 \mu M$) and HB-UC-6 ($IC_{50} = 0.158 \pm 0.38 \mu M$) were found potent than the standard compounds. In addition to that, these compounds were found to be non-toxic on the Vero cell line as these compounds did not show any significant inhibition (at least 50%) of the Vero cell line at $25 \mu M$.^[16] In case of stomach cancer (AGS) cell line; two compounds HB-UC-1 ($IC_{50} = 16.35 \pm 0.21 \mu M$) and HB-UC-10 ($IC_{50} = 23.06 \pm 0.21 \mu M$) were found to be most effective, while all standards Everolimus ($IC_{50} = 9.69 \pm 0.29 \mu M$), Cisplatin ($IC_{50} = 6.81 \pm 0.27 \mu M$), AZD-8055 ($IC_{50} = 5.73 \pm 0.54 \mu M$) and PI-103 ($IC_{50} = 1.46 \pm 0.22 \mu M$) showed good antiproliferative activity against stomach cancer cell line. In case of colon cancer cell line (HCT-15), compounds HB-UC-14 ($IC_{50} = 7.37 \pm 0.64 \mu M$), HB-UC-15 ($IC_{50} = 11.08 \pm 0.08 \mu M$), HB-UC-31 ($IC_{50} = 10.04 \pm 0.13 \mu M$), and HB-UC-37 ($IC_{50} = 12.24 \pm 0.12 \mu M$) were found to be effective. These compounds too were found to be non-toxic on the Vero cell line. In case of skin cancer cell line (B16F1), compounds like HB-UC-4 ($IC_{50} = 24.18 \pm 0.14 \mu M$), HB-UC-14 ($IC_{50} = 3.16 \pm 0.21 \mu M$) and HB-UC-33 ($IC_{50} = 17.41 \pm 0.23 \mu M$) were found to be effective. These compounds too were found to be non-toxic on the Vero cell line. Overall, six compounds; HB-UC-1, HB-UC-3, HB-UC-4, HB-UC-5, HB-UC-6 and HB-UC-9 were found to be most potent on the lung cancer cell line (A549) and were further used for various *in vitro* biological assays.

The present research work mainly deals with the treatment of lung cancer, hence efforts were made for description of the structure activity relationship of synthesized compounds with respect to MTT assay on lung cancer cell line.

In case of lung cancer cell line (A549), electronegative group at R_1 position was found to be effective for the antiproliferative activity. This was proved by the compounds of series-I where chlorobenzene group was present at R_1 position making this series of compounds effective as compared to the compounds of series-II and series-III where electronegative atoms were absent. Interestingly, in case of series-II, antiproliferative activity of compounds decreased drastically which proved the importance of polar functional group at R_1 and this results are in line with the outcome of 3D-QSAR study. In case of series-III, increased in the hydrophobicity at R_1 due to the alkyl side chain resulted in decreased antiproliferative activity against the lung cancer cell line (A549). Similar to the R_1 position, R_2 was also found to be favorable for the combination of hydrophobic group and polar functional group. This statements were proved by the

compounds HB-UC-1 ($IC_{50} = 0.06 \pm 0.27 \mu M$), HB-UC-4 ($IC_{50} = 0.971 \pm 0.16$) and HB-UC-5 ($IC_{50} = 0.224 \pm 0.45$), where compounds HB-UC-1 and HB-UC-5 consisted of the nitro ($-NO_2$) and amino ($-NH_2$) groups, respectively making R_2 position polar in nature compared to the compound HB-UC-4 where there was no polar functional group at R_2 . Additional validation to this statement was observed from the examples of the few other compounds viz. HB-UC-4 ($IC_{50} = 0.971 \pm 0.16$) and HB-UC-7 ($IC_{50} = 3.730 \pm 0.54$) where HB-UC-4 consisted of simple benzene ring at R_2 while on the other hand compound HB-UC-7 consisted of 4-methylbenzene which resulted into decreased in the polarity of compound HB-UC-7 compared to the HB-UC-4. During this enumeration of SAR, one interesting fact was observed in case of series-I that an increase in bulkiness without any proper polar functional groups at R_2 position decreased the activity against lung cancer cell line (A549). This was validated with an examples of the compounds viz. HB-UC-7 ($IC_{50} = 3.730 \pm 0.54$) and HB-UC-9 ($IC_{50} = 3.280 \pm 0.39$) where bulky groups like methyl ($-CH_3$) and (3,5-diCF₃) were present while in case of compound HB-UC-1 ($IC_{50} = 0.06 \pm 0.27$) and HB-UC-5 ($IC_{50} = 0.224 \pm 0.45$), the bulkiness at R_2 was found to be appropriate as compared to the compound HB-UC-7 and HB-UC-9 as these compounds HB-UC-1 and HB-UC-5 consisted of polar functional groups like nitro and amino, respectively.

Colony Forming Assay

Colony forming assay ^[26,27] is usually performed for observing the effect of the compounds on the uncontrolled cell proliferation of the cells. In lieu with this, six THQ derivatives viz. HB-UC-1, HB-UC-2, HB-UC-3, HB-UC-4, HB-UC-5 and HB-UC-9 which showed promising results against the lung cancer line (A549) were further taken for the colony forming assay. Three different concentrations of each compound i.e. 6.25 μM , 12.5 μM and 25 μM were used and it was observed that the compounds HB-UC-1 and HB-UC-5 showed a significant decrease ($p < 0.05$) in the colonies at 12.5 μM and 25 μM as compared to the DMSO control (results are shown in supporting information material as Figure SF-6A). The effect of one of the representative compound, HB-UC-1 on the colony formation is (depicted in supporting information material as Figure SF-6B), where it was observed that the number of colonies decreased depending on the concentration. Interestingly, compounds like HB-UC-3, HB-UC-4, HB-UC-6 and HB-UC-9 which showed good IC_{50} values against A549 cell line in MTT assay did not show any significant decrease in the colonies when three different concentrations of the compounds

were kept up to ten days in the contact of the A549 cell line. This experiment proved that the compounds HB-UC-3, HB-UC-4, HB-UC-6 and HB-UC-9 indicated promising IC₅₀ values in MTT assay when kept for 48 hours; but did not stop the uncontrolled cell growth of the A549 cells when a sufficient amount of media along with the nutrients were provided to the cells up to 10 days. Thus, only two compounds HB-UC-1 and HB-UC-5 were further used for screening. During this study it was observed that the compounds HB-UC-1 and HB-UC-5 showed a significant decrease ($p < 0.05$) in the colonies at 12.5 μM and 25 μM compared to the DMSO control as shown in supporting information material. Thus, only two compounds HB-UC-1 and HB-UC-5 were further used for screening.

Cell Apoptosis Assay

In the present research work for determination of apoptosis - FACS (Fluorescence-Activated Cell Sorting) analysis was carried with the aid of flow cytometry [28,29]. For this study, compounds HB-UC-1 and HB-UC-5 (two concentrations of each; 3 and 6 μM) along with the standard Everolimus (6 μM) were selected, as both compounds showed promising activity in enzyme, MTT and colony forming assay. This analysis revealed the apoptotic properties of Everolimus, HB-UC-1 and HB-UC-5 as compared to DMSO as control (Shown in Figure 3(A) to 3(F)). In case of Everolimus (6 μM) and the compound HB-UC-1 (6 μM), 40.09 % and 53.97 % of the cells were found in late apoptotic phase, respectively. This percentage of late apoptosis of compound HB-UC-1 decreased at 3 μM . Similarly, in the case of the compound HB-UC-5 (6 μM), 36.13% of the cells were found in late apoptosis which was less as compared to the standard, Everolimus. This study also concluded that both these compounds were non-necrotic, as a negligible amount of cells were found to be in necrotic phase. Overall, this analysis demonstrated the apoptotic properties of compound HB-UC-1 and HB-UC-5. Moreover this study also indicated that both the compounds HB-UC-1 and HB-UC-5 were apoptosis inducer but the compound HB-UC-1 at 6 μM was one of the best apoptotic inducers compared to Everolimus.

Gene Expression Study

For gene expression study [30,31], isolated RNA samples were selected as they remained intact after the treatment of compound HB-UC-1 (0.06 μM) and HB-UC-5 (0.11 μM), at their IC₅₀ concentration as shown in Figure 4 (A). The cDNA form of the cells treated with the compounds at their IC₅₀ and control was used as a template for further gene amplification with the use of gene-specific primer E4BP4.

Among these two compounds, HB-UC-1 showed some promising effect as it reduced the expression level of the E4BP4 as shown in Figure 4(B) and 4(C) which indicated that the compound HB-UC-1 was inhibiting the mTORC1 expression. Although it is well known that the E4BP4 gene is involved in many other pathways like MEK/ERK, PKA/PTH/FSK, GR/CREB pathways, hence it was difficult to conclude that the compound is inhibiting the mTORC1. Hence, to overcome the above-mentioned problem of E4BP4 which is not a specific downstream regulator of mTORC1; a primer of specific downstream regulators of mTORC1 and mTORC2 were used viz. eIF4EBP1 and PCK1, respectively. eIF4EBP1 had both antioncogenic and proapoptotic properties and hence it was involved in the normal cellular process.

Usually, the expression of eIF4EBP1 was decreased due to increased expression of mTORC1 as it was a natural inhibitor of eIF4EBP1. Hence, if there was an inhibition of mTORC1, it could lead to increased expression level of the eIF4EBP1 which is good for the normal cellular process. The cDNA of cells, treated with the HB-UC-1 were taken and amplified through eIF4EBP1 primers and it was observed that the expression level of the eIF4EBP1 was increased as shown in Figure 4(D) and 4(E) which indicated that the compound HB-UC-1 inhibited the mTORC1. Similarly, PCK1 was presented downstream to the protein mTORC2. PCK1 was responsible for the augmentation of the gluconeogenesis which consequently lead to uncontrolled cell proliferation. Hence, inhibition of the mTORC2 resulted in decreased expression of the PCK1 as shown in Figure 4(D) and 4(F). Compound HB-UC-1 increased the expression level of eIF4EBP1 which proved that this compound inhibited the mTORC1 efficiently. Similarly, compound HB-UC-1 completely decreased the expression level of PCK1 which demonstrated the effectiveness of this compound as mTORC2 inhibitor. Overall, gene expression study revealed that the compound HB-UC-1 was found as effective mTOR inhibitor (both mTORC-1 and mTORC-2).

Western Blot Analysis

Gene expression study clearly revealed the mTORC1 and mTORC2 inhibitory activity of compound HB-UC-1. Additionally to know the indirect mTORC1 inhibition via AKT and direct mTORC2 inhibition by compounds HB-UC-1 and HB-UC-5, western blot analysis [32,33] was carried out and depicted in Figure 4(G) and 4(H). AKT is serine/threonine protein kinase which is a downstream regulator of

mTORC2 protein. Hence, inhibition of the phosphorylation of AKT S473 gave an idea about the mTORC2 inhibition. pAKT directly inhibited downstream regulating protein viz. Glycogen Synthase Kinase 3 (GSK3), FoxO (FOXO) which consequently resulted into suppression of apoptotic signals and lead to uncontrolled cell proliferation. In addition to this, AKT indirectly activated the mTORC1, which further resulted into the cell proliferation. This indirect activation of mTORC1 usually took place through the phosphorylation of the TSC1/2 which resulted into the increment in the activity of mTORC1; hence, inhibition of phosphorylation of AKT indirectly decreased the activity of mTORC1. Both these compounds were evaluated at four different concentration ranging from 0.1 μ M to 5 μ M. These compounds showed significant inhibition of pAKT S473 at mentioned concentrations compared to the control (0 μ M) as these compounds inhibited the downstream protein regulator of mTORC2 (pAKT S473) in the lung cancer cell line (A549). These compounds block the phosphorylation of the AKT at S473 site depending on the concentration as shown in Figure 4(G) and 4(H). This inhibition of the phosphorylation of AKT at S473 site also proved that these compounds HB-UC-1 and HB-UC-5 were useful for the prevention of feedback activation of AKT in the lung cancer cell line (A549) which consequently lead to activation of mTORC1. Hence, inhibition of pAKT proved the efficiency of compounds HB-UC-1 and HB-UC-5 as a direct mTORC2 inhibitor and indirect mTORC1 inhibitor.

Reported rapalogues unable to inhibit the mTORC2 due to their structural arrangements which were different from the mTORC1. mTORC-2 consist of Rictor-mSin-1 complex instead of Raptor which was the only difference between the mTORC-1 and mTORC-2. These Rictor-mSin-1 complex generated steric hindrance to the Rapamycin-FKBP12 complex which resulted into the insensitivity of mTORC-2 protein toward the rapamycin and rapalogs. In the present research work, efforts were made to design and synthesize small molecules which were not repelled by the steric hindrance of the Rictor-mSin-1 of mTORC2 complex. The western blot analysis of compound HB-UC-1 and HB-UC-5 showed that these compounds HB-UC-1 and HB-UC-5 inhibited the phosphorylation of AKT S473 which proved the efficiency of this compounds as mTORC2 inhibitors. It also ascertained that these compounds prevent the indirect activation of mTORC1 via AKT. Hence, this study demonstrated that the compounds HB-UC-1 and HB-UC-5 were inhibited both mTORC1 and mTORC2 which is a major advantage of these compounds over the rapalogs.

***In-Vivo* Biological Evaluation**

Detailed *in-vitro* biological evaluation of novel THQ derivatives concluded compounds HB-UC-1 and HB-UC-5 as most effective and potent against the lung cancer through inhibition of mTOR enzyme. Based upon this evaluations, compounds HB-UC-1 and HB-UC-5 were further selected to evaluate their efficacy on life span and lung cancer animal models. In case of lung cancer animal model, Everolimus was selected as a standard drug for the comparison.^[34-35]

Lifespan Animal Model

For the initial evaluation, a study was performed using the compounds HB-UC-1 and HB-UC-5 to evaluate the effect on the life span of the cancer-bearing animals.^[36] P388D1 leukemia cells were given intraperitoneally to the mice for the induction of the cancer and observation was made for the 30 days where throughout the experiment, deaths of animals were recorded. Life span study clearly revealed that on the 15th day, all animals in the diseased control group died as shown in Table 2 (also expressed as supporting information material Figure SF-7). While in case of compounds HB-UC-1 and HB-UC-5, animals were survived on and after 22nd day as shown in (supporting information material as Figure SF-7) and Table 2, respectively. In the case of compound HB-UC-1, the mean survival time of the animals increased with 83% survival rate as compared to the diseased control group as shown in Table 2. While with HB-UC-5, the mean survival time of the animals increased compared to the disease control group but the percent rate of survival was observed to be only 16% as shown in Table 2.

In conclusion, the compound HB-UC-1 was found to be very much effective and safe with the mentioned dose. Additionally, it increased the lifespan of the animals with a good survival rate. The compound HB-UC-5 showed some promising result by increasing the lifespan of the animals but the percentage of survival was found to be less in this treatment group compared to the HB-UC-1 group. Therefore further these two molecules were taken for *in-vivo* analysis in the lung cancer animal model.

Lung Cancer Animal Model

After the accomplishment of efficacy in lifespan animal model, compounds HB-UC-1 and HB-UC-5 were assessed against the benzo[a]pyrene induced lung cancer animal model.^[37-39] (Mechanism of induction of lung cancer through the Benzo(a)pyrene is provided as supporting information material Figure SF-8.) Various parameters like body weight and lung weight, serum biomarkers and histopathological studies were determined in detail to prove effectiveness of synthesized compounds.

Initially, lung cancer was induced in mice with the help of benzo[a]pyrene which is a nicotine analogue. Benzo[a]Pyrene (50mg/kg body weight) was dissolved in olive oil and given twice a week for four consecutive weeks. Standard drug, Everolimus & two drugs, HB-UC-1 and HB-UC-5 were given thrice a week to the animals after the induction of lung cancer i.e. after the 8th week. The treatment started in the 9th week and continued up to the 16th week. It was observed that on the 16th week, body weight of disease control animal declined significantly ($P < 0.05$) compared to the normal control. All the animals were euthanized by cervical dislocation after the 16th week with the help of ether anesthesia. Lungs of all animals were removed and weighed. Lung weight was increased significantly ($P < 0.05$) compared to the normal control group. This decreased in the body weight occurred due to the weaker immunity which resulted due to the induction of the lung cancer while increment in the weight of lungs clearly indicated occurrence of the tumor in the lungs.

Body Weight and Lung Weight Analysis

Usually, an induction of lung cancer resulted in reduction of the body weight while on the other hand, it increased lung weight due to the formation of the tumor. In line with this, in the present research, it was observed in diseased control group that after the 5th week, there was a slight decline in the body weight of mice which consequently declined each week. After the completion of the experiment, on the 16th week, it was observed that the body weight of disease control animal declined significantly ($P < 0.05$) compared to the normal control, as shown in Table 3. On the other hand, in the case of treatment group, recovery in body weight was observed which is shown in Table 3. Group of animals treated with both compounds HB-UC-1 and HB-UC-5 showed significant recovery in the body weight with compound HB-UC-1 showed significant ($p < 0.05$) effect and was found to be more effective along with the standard drug

Everolimus as shown in Table 3. The same pattern was observed in the lung weight which increased significantly ($p < 0.05$) in diseased control group due to the tumor formation in the lung. While in the treatment group, the lung weight decreased significantly ($p < 0.05$) which was primarily indicated the reduction in the tumors. Overall, Everolimus, HB-UC-1 and HB-UC-5 were found to be effective as a significant ($p < 0.05$) difference in the lung weight in the treatment groups were observed compared to the diseased control group.

Serum Biomarkers

An abrupt increment in the pyruvate in the serum indicated the uncontrolled cell growth compared to the normal which consequently happened due to increase in the lactate dehydrogenase (LDH). In the present research work, statistical results and its graphical representation, as shown in Figure 5 (A), indicated that the LDH level significantly increased ($P < 0.05$) in disease control group as compared to normal control (NC) group which confirmed the tumor formation in the mice. In the treatment groups, the LDH level was found to be significantly less ($P < 0.05$) than the diseased control (DC) group which indicated the effectiveness of the treatment.

Similar to LDH level, the statistical results of GGT level along with its graphical representation (Figure 5(B)) indicated a significant ($P < 0.05$) increase in the GGT level in the diseased control group compared to the normal control group. Although, the treatment group indicated a significant reduction in the GGT level ($P < 0.05$). Everolimus and HB-UC-1 treated groups showed the GGT level almost near to the normal control group.

Overall, Serum biomarkers viz. Lactate Dehydrogenase (LDH), Gamma Glutamyl Transferase (GGT) increased significantly in the disease control group indicated the induction of tumor while in case of treatment group the level of Lactate Dehydrogenase (LDH), Gamma Glutamyl Transferase (GGT) decreased significantly indicated effectiveness of these two compounds HB-UC-1 and HB-UC-5 against the lung cancer.

Biomarkers of Tissue Homogenate

Malondialdehyde (MDA) is a product of the lipid peroxidation which occurred due to the reaction between the free radical and lipid. This MDA is responsible for the DNA base pair mutation which consequently leads to the uncontrolled cell proliferation. A significant increase in level of MDA ($P < 0.05$) in the diseased control group was observed as compared to the normal control group which indicated about lipid peroxidation (as shown in Figure 5(C)). But on the other hand, in the treatment groups, significant ($P < 0.05$) reduction in MDA level was observed. HB-UC-1 and HB-UC-5 were found to be as effective as the standard drug Everolimus as it reduced the MDA level significantly ($P < 0.05$).

Glutathione is considered as one of the most important antioxidants of the human body. If there is an increase in the free radicles formation in the body, Glutathione helps in the reduction of the oxidative stress which is usually generated due to this free radicle formation. But as there is an enormous amount of free radicles like in carcinogenesis, it could lead to a reduction in the level of Glutathione. The level of Glutathione when significantly reduced ($P < 0.05$) in the diseased control group compared to the normal control group indicated the enormous free radical generation due to the cancer induction as shown in Figure 5 (D). But in the case of treatment groups, viz. Everolimus and HB-UC-1, the level of glutathione was increased indicating the potency of these two compounds as a free radical scavenger which helped to maintain the glutathione level at normal. Compound HB-UC-5 also showed some antioxidant property as in this group, a higher level of glutathione was observed compared to the diseased control group.

Catalase is one of the important cellular antioxidants which reduces the cellular damage due to the oxidative stress. Results of the catalase activity is shown in Figure 5 (E) which indicated that the level of hydrogen peroxide consumption decreased in the disease control group compared to the normal control due to the decrease in the catalase enzyme activity. This clearly indicated the presence of oxidative stress in the disease control group compared to the normal control group. But this catalase activity was significantly ($P < 0.05$) increased in the Everolimus treatment group which indicated the very high consumption of peroxide free radicals. Similarly, HB-UC-1 and HB-UC-5 also showed some antioxidant activity as there was an increment in the catalase activity and more consumption of hydrogen peroxide free radicals.

Overall, a significant level of Malondialdehyde level was increased ($P < 0.05$) in the diseased control group compared to the normal control group which indicated about lipid peroxidation. But on the other hand, in the treatment groups, significant ($P < 0.05$) reduction of the Malondialdehyde level was observed. This outcome clearly indicated that the compounds HB-UC-1 and HB-UC-5 reduced the lipid peroxidation effectively. A reduction in the level of Glutathione in diseased control group proved that the enormous amount of free radicles were generated in it. However treatment group indicated the significant increment of the glutathione level which established the antioxidant properties of compound HB-UC-1 and HB-UC-5. Decreased in the catalase activity in the disease control group indicated the production of free radicles. Generation of these free radicles occurred due to the induction of the lung cancer. Nevertheless treatment with the compounds HB-UC-1 and HB-UC-5 showed higher level of the catalase activity compared to the diseased control group confirmed the free radicle scavenging properties of the these compounds which consequently helped for the treatment of the lung cancer.

Histopathological Study

Histopathological evaluation of lung tissue was carried out to access the induction of tumor and effectiveness of the synthesized compounds along with the standard drug Everolimus. Lungs' photographs and their histopathological evaluation is depicted in Figure 5(F) and 5(G), respectively. This study proved the effect of compound HB-UC-1 and HB-UC-5 as it indicated the difference in morphology of lung tissue between the normal control (NC), disease control (DC) and treatment groups. Lung section of a mice from the normal control group indicated the proper structure of alveoli. In addition to this, it also showed the uniformity in the nuclei. In the case of disease control group, the hyperchromatic nuclei were found on the walls of alveolar cells and an enormous amount of alveolar damage was observed which is shown in Figure 5(G). While treatment groups which involved the treatment of Everolimus, HB-UC-1, HB-UC-5 showed very less damage to the alveoli. Additionally, a few hyperchromatic nuclei observed in these sections proved the efficacy of the compound HB-UC-1 and HB-UC-5.

Overall, measurement of the various biochemical parameters like Lactate Dehydrogenase (LDH), Gamma Glutamyl Transferase (GGT), Catalase (CAT), Malondialdehyde (MDA) along with the histopathological evaluation of the lungs of the mice revealed that both the

compounds HB-UC-1 and HB-UC-5 cured the lung cancer up to some extent in the mice as compared to the standard molecule viz. Everolimus.

Conclusion

The research work was started with understanding of target receptor for binding interactions which gave deep insights for incorporation of substitutions in designed molecules which was supported by 3D-QSAR studies. It was followed by rationale drug design process by pharmacophore based virtual screening to conclude THQ as core scaffold. Finally, based upon molecular docking studies, 31 novel tetrahydroquinoline derivatives were designed and synthesized. The structures of these synthesized tetrahydroquinoline derivatives confirmed by FTIR, ^1H & ^{13}C NMR and Mass. Finally, XRD analysis proved designed series. HPLC analysis gave idea about purity of synthesized compounds which was >95% for all compounds. To evaluate synthesized compounds for their anticancer potential, various *in-vitro* and *in-vivo* analysis was performed. *In-vitro* biological evaluation of these 31 derivatives was carried out through mTOR enzyme assay and MTT assay on various cancer cell lines which gave six compounds as potential target for further studies. Colony forming assay further helped to narrow down on two compounds, HB-UC-1 & HB-UC-5, for flow cytometry analysis, gene expression study and western blot analysis. Both compounds showed their potency in all studies. From results of all *in-vitro* analysis, both compounds were further investigated for *in-vivo* biological evaluation. Both molecules, HB-UC-1 and HB-UC-5, showed promising results in the life span animal model and benzo[a]pyrene induced lung cancer animal model. These designed molecules could be further explore in future as HITs to develop novel Lead molecule for the treatment of Lung cancer.

Experimental Section

Material and Methods

For the synthesis of these designed THQ derivatives suitable synthetic scheme was designed which is depicted in Figure 2. Borosilicate glassware and dry solvents were utilized for the synthesis of all the intermediates along with the final desired compounds. There were certain steps in the synthetic scheme where heating and stirring were required which was done with the aid of REMI Rota-mantle.

Solvents were evaporated with the help of BUCHI type rotary vacuum evaporator. Synthesized products were dried under the IR lamp for an appropriate time duration. After drying all synthesized compounds were taken for melting point determination with the help of VEEGO corporation melting point apparatus and are uncorrected. All the thirty one tetrahydroquinoline derivatives were purified using column chromatography and further their purity was confirmed with the help of JASCO HPLC instrument and all compounds gave >95% purity. These all tetrahydroquinoline derivatives were characterized with the help of Infrared Spectroscopy (JASCO 6100), Mass Spectroscopy (WATERS Mass Spectrometer), ^1H NMR and ^{13}C NMR (BRUKER AVANCE-II). For the accurate confirmation and validation of spectral data; X-ray crystallography of one of the compound HB-UC-25 of the series was carried out with the help of RIGAKU SCX mini diffractometer.

Experimental Procedure and Spectral Characterization of Intermediates

Synthesis of (9H-fluoren-9-yl) methyl-3,4-dihydroquinoline-1(2H)-carboxylate (3):

THQ (**1**) (3.75 mmol, 0.47 mL) and Fmoc (**2**) (4.125 mmol, 1.06 gm) were dissolved in the dichloromethane with continued stirring at 0°C . Dropwise addition of trimethylamine (4.125 mmol, 0.5 mL) was carried out to above reaction mixture with continuous stirring at 0°C . Allow reaction mixture to stir at room temperature for 24 hours. Solvent was evaporated and the desired product was dissolved in the ethyl acetate. This product was extracted with the dilute HCl to remove the excess trimethylamine and Fmoc. Finally washing was done with the brine solution and ethyl acetate was evaporated to get the desired white colored product. Yield: 69 %; mp: $88-90^\circ\text{C}$; IR (KBr, $\gamma_{\text{max}} \text{ cm}^{-1}$): 1577 (C=O), 1710 (C=C), 2360 (C-N), 2942 (C-H aliphatic), 3034 (C-H aromatic); MS (EI) m/z calculated for $\text{C}_{24}\text{H}_{21}\text{NO}_2$ 356 (M+1), found 356 (M+1).

Synthesis of (9H-fluoren-9-yl) methyl 6-nitro-3,4-dihydroquinoline-1(2H)-carboxylate (4):

Nitrating mixture was made with the help of KNO_3 (1000 mmol, 0.142 gm) and H_2SO_4 (1000 mmol, 0.074 mL) and allow to stir at 0°C for 10 to 15 minutes. Addition of dichloromethane was carried out to above reaction mixture at 0°C and again allowed to stir above

reaction mixture for 15 minutes. (9H-fluoren-9-yl)methyl-3,4-dihydroquinoline-1(2H)-carboxylate (**3**) (1000 mmol, 0.5 gm) was dissolved in dichloromethane and added dropwise to above reaction mixture while temperature was maintained at 0°C. Continued stirring of reaction mixture for 2 hours and 30 minutes at RT. Poured reaction mixture to the crushed ice and product was extracted with dichloromethane followed by washing with brine resulted into yellow color product. Yield: 96 %; mp: 140-142°C; IR (KBr, γ_{max} cm⁻¹): 1585(C=O), 1706(C=C), 2350(C-N), 2944(C-H aliphatic), 3098(C-H aromatic); MS (EI) m/z calculated for C₂₄H₂₀N₂O₂ 401 (M+1), found 418 (M+18).

Synthesis of 6-nitro tetrahydroquinoline (5):

Compound **4** (1000 mmol, 3 gm) was dissolved in dichloromethane. Pyrrolidine (3000 mmol, 1.8 mL) was added dropwise to above reaction mixture and allowed to stir the reaction mixture for 15 to 30 minutes. Poured mixture to crushed ice and desired product was extracted with dichloromethane. Finally the product was washed with the brine and dried over sodium sulfate resulted into the dark yellow color product. Yield: 85 %; mp: 160-162°C; IR (KBr, γ_{max} cm⁻¹): 1609 (C=C), 2359 (C-N), 2962 (C-H aliphatic), 3063 (C-H aromatic); MS (EI) m/z calculated for C₉H₁₀N₂O₂ 179 (M+1), found 179.4 (M+1).

Synthesis of (4-chlorophenyl)(6-nitro-3,4-dihydroquinolin-1(2H)-yl)methanone (7a):

Compound **5** (1000 mmol, 0.2 gm) was dissolved in dichloromethane and dropwise addition of trimethylamine (1000 mmol, 0.16 mL) was carried out to above reaction mixture with continues stirring. The reaction mixture was allowed to stir for 30 minutes followed by the addition of 4-chloro benzoyl chloride (**6a**) (1000 mmol, 0.14 mL). This reaction mixture was kept on stirring at room temperature for 24 hours consequently this mixture was added to the crushed ice and extracted with the dichloromethane. Further it was washed with the bicarbonate solution, brine and dried over sodium sulfate resulted into the light yellow color powder. Yield: 84 %; mp: 170-173°C; IR (KBr, γ_{max} cm⁻¹): 1667(C=O), 1786(C=C), 2360(C-N), 2954(C-H aliphatic), 3095(C-H aromatic); MS (EI) m/z calculated for C₁₆H₁₃ClN₂O₃ 317 (M+1), found 317 (M+1) and 319.3 for chloro pattern.

Synthesis of (6-nitro-3,4-dihydroquinolin-1(2H)-yl)(phenyl)methanone (7b):

Procedure of synthesis of this compound **7b** remained same as that of the synthesis of the compound **7a** only difference was that the benzoyl chloride (**6b**) was used instead of 4-chloro benzoyl chloride (**6a**). Yield: 86 %; mp: 168-170°C; IR (KBr, γ_{\max} cm^{-1}): 1665(C=O), 1784(C=C), 2356(C-N), 2953(C-H aliphatic), 3015(C-H aromatic); MS (EI) m/z calculated for $\text{C}_{16}\text{H}_{14}\text{ClN}_2\text{O}_3$ 283, found 283 (M+1).

2-ethyl-1-(6-nitro-3,4-dihydroquinolin-1(2H)-yl)butan-1-one (7c):

Procedure of synthesis of this compound **7c** remained same as that of the synthesis of the compound **7a** only difference was that the aliphatic 2-ethyl butanoyl chloride (**6c**) was used instead of 4-chloro benzoyl chloride (**6a**).

Synthesis of (6-amino-3,4-dihydroquinolin-1(2H)-yl)(4-chlorophenyl)methanone (8a):

The mixture of ammonium chloride (7000 mmol, 0.5 gm) was prepared in water: methanol (3:7). Simultaneously the compound **7a** (1000 mmol, 0.3 gm) was added to suitable quantity of methanol followed by the addition of the zinc dust (10000 mmol, 0.43 gm). The above mixture of ammonium chloride was poured into this reaction mixture of compound and zinc dust. This reaction mixture was allowed to stir at 60 °C for 6 hours resulted into the reduction of nitro group to amine. Further methanol was evaporated and the mixture was dissolved in the ethyl acetate and extracted with bicarbonate. The compound was dried over the sodium sulfate. Yield: 80 %; mp: 190-193°C; IR (KBr, γ_{\max} cm^{-1}): 1552(C=O), 1600(C=C), 2360(C-N), 2931(C-H aliphatic), 3361(C-H aromatic); MS (EI) m/z calculated for $\text{C}_{16}\text{H}_{15}\text{ClN}_2\text{O}$ 287 (M+1), found 287.5 (M+1) and 289.5 for chloro pattern.

Synthesis of (6-amino-3,4-dihydroquinolin-1(2H)-yl)(phenyl)methanone (8b):

Procedure of synthesis of this compound remained same as that of the synthesis of the compound **8a**, only difference was that the **7b** was used instead of **7a**. Yield: 79 %; mp: 189-192°C; IR (KBr, γ_{\max} cm^{-1}): IR (KBr, γ_{\max} cm^{-1}): 1550(C=O), 1601(C=C), 2360(C-N), 2935(C-H aliphatic), 3363(-NH₂), 3366(C-H aromatic); MS (EI) m/z for $\text{C}_{16}\text{H}_{16}\text{N}_2\text{O}$ 251, found 251 (M+1).

1-(6-amino-3,4-dihydroquinolin-1(2H)-yl)-2-ethylbutan-1-one (8c):

Procedure of synthesis of this compound **8c** remained same as that of the synthesis of the compound **8a**, only difference was that the compound **7c** was used instead of **7a**.

Synthesis and Spectral Characterization of Final Derivatives (Series-I):

Synthesis of (N-(1-(4-chlorobenzoyl)-1,2,3,4-tetrahydroquinolin-6-yl)-4-nitrobenzamide: (HB-UC-1) (9d):

Compound **8a** (1.7 mmol, 0.5 gm) was dissolved in the dichloromethane. Dropwise trimethylamine (4.9 mmol, 0.46 mL) was added to above reaction mixture and allowed to stir for 30 minutes at room temperature. 4-nitro benzoyl chloride (1.6 mmol, 0.3 gm) was added to above reaction mixture and stirring was continued for 1 hour. Reaction mixture was transferred to the crushed ice and extracted with dichloromethane dried over the sodium sulfate and passed through the column for the purification resulted into yellow colored compound. Dark yellow Solid Yield: 65.78 %; mp: 206-208°C; IR (KBr, γ_{\max} cm^{-1}): 843 (C-Cl), 1530 (-NO₂), 1599 (C=O), 1673 (C=C), 2360 (C-N), 2951 (C-H aliphatic), 3015 (C-H aromatic), 3319 (-NH); ¹H NMR (400 MHz, DMSO-d₆) δ PPM: 1.95-1.98 (m, 2H, -CH₂), 2.82 (t, J = 5.6 Hz, 2H, -CH₂), 3.76 (m, 2H, -CH₂), 6.74 (s, 1H, Ar-CH), 7.26 (d, J = 8 Hz, 1H, Ar-CH), 7.35 (d, J = 8 Hz, 2H Ar-CH), 7.42 (d, J = 8 Hz, 2H, Ar-CH), 7.71 (s, 1H, Ar-CH), 8.14 (d, J = 8.4 Hz, 2H, Ar-CH), 8.35 (d, J = 8.4 Hz, 2H, Ar-CH), 10.49 (s, 1H, NH-C=O); ¹³C NMR (100 MHz, DMSO-d₆) δ PPM: 23.48, 26.48, 44.26, 117.74, 120.16, 123.53, 125.14, 128.23(2C), 128.43(2C), 129.09(2C), 129.50(2C), 130.09, 131.91, 134.52, 135.09, 140.47, 149.08, 163.50, 167.97; MS (EI) m/z calculated for C₂₃H₁₈ClN₃O₄ 436 for (M+1); found 436.4 (M+1), 438.4 (for chloro pattern); HPLC Purity: 97.58%.

Synthesis of 4-chloro-N-(1-(4-chlorobenzoyl)-1,2,3,4-tetrahydroquinolin-6-yl)benzamide (HB-UC-2) (9e):

The procedure remained same as that of the compound **9d**, only instead of 4-nitro benzoyl chloride; 4-chloro benzoyl chloride (1.7 mmol, 0.23 mL) was added. Pale yellow Solid Yield: 67.56 %; mp: 230-232°C; IR (KBr, γ_{\max} cm^{-1}): 842 (C-Cl), 1599 (C=O), 1662 (C=C), 2360 (C-N), 2934(C-H aliphatic), 3071 (C-H aromatic), 3340 (-NH); ¹H NMR (400 MHz, DMSO-d₆) δ PPM: 1.95-1.98 (m, 2H,-CH₂), 2.80-2.83 (m, 2H,-CH₂), 3.75-3.77 (m, 2H, -CH₂), 6.71 (m, 1H, Ar-CH), 7.26-7.28 (m, 1H, Ar-CH), 7.35 (d, 2H, J = 8 Hz, Ar-CH), 7.41 (d, 2H, J = 8 Hz, Ar-CH), 7.56-7.58 (m, 2H, Ar-CH), 7.61 (m, 2H, Ar-CH), 7.71 (s, 1H, Ar-CH), 10.29 (s, 1H, NH-C=O);

^{13}C NMR (100 MHz, DMSO- d_6) δ PPM: 23.50, 26.58, 40.08, 117.68, 128.22, 128.41, 128.72, 128.93 (2C), 129.53 (2C), 131.81 (2C), 132.25 (2C), 134.48, 135.34, 135.41, 136.33, 137.15, 140.17, 164.15, 167.92; MS (EI) m/z calculated for $\text{C}_{23}\text{H}_{18}\text{ClN}_2\text{O}_2$ 425 for (M+1); found 425.3 (M+1), 427.4 (for chloro pattern); HPLC Purity: 96.93%.

Synthesis of 4-bromo-N-(1-(4-chlorobenzoyl)-1,2,3,4-tetrahydroquinolin-6-yl)benzamide (HB-UC-3) (9f):

The procedure remained same as that of the compound **9d**, only instead of 4-nitro benzoyl chloride; 4-bromo benzoyl chloride (1.2 mmol, 0.27 gm) was used. Pale yellow Solid Yield: 82.71 %; mp: 201-206°C; IR (KBr, γ_{max} cm^{-1}): 843 (C-Cl), 1594 (C=O), 1682 (C=C), 2360 (C-N), 2934 (C-H aliphatic), 3081 (C-H aromatic), 3337 (-NH); ^1H NMR (400 MHz, DMSO- d_6) δ PPM: 1.96 (m, 2H, -CH₂), 2.82 (m, 2H, -CH₂), 3.75 (m, 2H, -CH₂), 6.71 (s, 1H, Ar-CH), 7.26-7.73 (m, 8H, Ar-CH), 7.88 (m, 2H, Ar-CH), 10.24 (s, 1H, NH-C=O); ^{13}C NMR (100 MHz, DMSO- d_6) δ PPM: 23.49, 26.48, 44.25, 117.67, 120.07, 125.29, 128.21, 128.42(2C), 129.68(2C), 130.08(2C), 131.36(2C), 131.83, 133.86, 134.49, 135.38, 136.20, 164.26, 167.92; MS (EI) m/z calculated for $\text{C}_{23}\text{H}_{18}\text{BrClN}_2\text{O}_2$ 469 (M+1), found 469.3 (M+1), 471.2 (for bromo chloro pattern), 473.3 (for bromo chloro pattern); HPLC Purity: 96.96%.

N-(1-(4-chlorobenzoyl)-1,2,3,4-tetrahydroquinolin-6-yl)benzamide (HB-UC-4) (9g):

The procedure remained same as that of the compound **9d**, only instead of 4-nitro benzoyl chloride; benzoyl chloride (1.7 mmol, 0.19 mL) was used. White Solid Yield: 85.29 %; mp: 196-198°C; IR (KBr, γ_{max} cm^{-1}): 843 (C-Cl), 1598 (C=O), 1671 (C=C), 2360 (C-N), 2944 (C-H aliphatic), 3324 (-NH), 3036 (C-H aromatic); ^1H NMR (400 MHz, DMSO- d_6) δ PPM: 1.96 (m, 2H, CH₂), 2.80 (t, J = 6 Hz, 2H, -CH₂), 3.76 (m, 2H, -CH₂), 6.70 (s, 1H, Ar-CH), 7.27 (d, J = 8 Hz, 1H, Ar-CH), 7.35 (d, J = 8.4 Hz, 2H, Ar-CH), 7.41 (d, J = 8.4 Hz, 2H, Ar-CH), 7.50 (m, 1H, Ar-CH), 7.56 (t, J = 7.2 Hz, 2H, Ar-CH), 7.74 (s, 1H, Ar-CH), 7.93 (d, J = 7.2 Hz, 2H, Ar-CH), 10.21 (s, 1H, NH-C=O); ^{13}C NMR (100 MHz, DMSO- d_6) δ PPM: 23.52, 26.50, 44.23, 117.62, 120.01, 125.05, 127.56, 128.21, 128.33(2C), 129.53(2C), 130.10(2C), 131.49(2C), 134.31, 134.49, 134.84, 135.36, 135.65, 165.30, 167.91; MS (EI) m/z calculated for $\text{C}_{23}\text{H}_{19}\text{ClN}_2\text{O}_2$ 391 (M+1), found 391.4 (M+1), 393.4 (for chloro pattern); HPLC Purity: 96.93%.

4-Amino-N-(1-(4-chlorobenzoyl)-1,2,3,4-tetrahydroquinolin-6-yl)benzamide (HB-UC-5) (9h):

Initially compound **9d** was synthesized as per the procedure mentioned above and further reduction was carried out as per the procedure of synthesis of compound **8a**, only instead of compound **7a**; compound **9d** was used with 10 equivalent zinc and 7 equivalent ammonium chloride. Pale yellow Solid Yield: 92.85%; mp: 210-214°C; IR (KBr, γ_{max} cm⁻¹): 840 (C-Cl), 1506 (C=O), 1622 (C=C), 2360 (C-N), 2854 (C-H aliphatic), 2931 (C-H aromatic), 3044 (-NH), 3333 (-NH₂); ¹H NMR (400 MHz, DMSO-d₆) δ PPM: 1.94 (t, 2H, J = 6.4 Hz, -CH₂), 2.78-2.81 (m, 2H, -CH₂), 3.73 (t, 2H, J = 6 Hz, -CH₂), 5.75 (s, 1H, -NH), 6.60 (s, 1H, Ar-CH), 6.57 (d, 2H, J = 8.4 Hz, Ar-CH), 7.21 (d, 2H, J = 8.4 Hz, Ar-CH), 7.34 (d, 2H, J = 8.4 Hz, Ar-CH), 7.40 (d, 2H, J = 8.4 Hz, Ar-CH), 7.67 (d, 2H, J = 8 Hz, Ar-CH), 9.67 (s, 1H, NH-C=O); ¹³C NMR (100 MHz, DMSO-d₆) δ PPM: 23.55, 26.50, 44.25, 117.32, 119.67, 120.92, 124.95, 128.19 (2C), 128.43 (2C), 128.62 (2C), 129.24 (2C), 130.09, 131.75, 133.63, 134.42, 135.42, 152.09, 165.06, 167.82; MS (EI) m/z calculated for C₂₃H₂₀ClN₃O₂ 405 (M+1), found 405.9 (M+1), 407.7 (for chloro pattern); HPLC Purity: 96.21 %.

Ethyl 2-(1-(4-chlorobenzoyl)-1,2,3,4-tetrahydroquinolin-6-ylamino)-2-oxoacetate (HB-UC-6) (9i):

The procedure remained same as that of the compound **9d**, only instead of 4-nitro benzoyl chloride; ethyl 2-chloro-2-oxoacetate (0.8 mmol, 0.18 mL) was taken. Pale yellow Solid Yield: 66.58 %; mp: 190-192°C; IR (KBr, γ_{max} cm⁻¹): 833 (C-Cl), 1534 (C=O), 1695 (C=C), 2360 (C-N), 2931 (C-H aliphatic), 3063 (C-H aromatic), 3394 (-NH); ¹H NMR (400 MHz, DMSO-d₆) δ PPM: 1.29 (m, 3H, -CH₃), 1.93 (m, 2H, -CH₂), 2.78 (m, 2H, -CH₂), 3.72 (m, 2H, -CH₂), 4.29 (m, 2H, -CH₂), 7.38-7.65 (m, 7H, Ar-CH), 10.71 (s, 1H, NH-C=O); ¹³C NMR (100 MHz, DMSO-d₆) δ PPM: 13.80, 23.40, 28.45, 44.29, 62.34, 117.72, 120.09 (2C), 125.16, 128.23, 130.09(2C), 131.91(2C), 133.86, 134.56, 135.22, 155.27, 160.57, 168.02; MS (EI) m/z calculated for C₂₀H₁₉ClN₂O₄ 387 (M+1), found 404.0 (M+18 for water adduct) 406.0 (M+20 for chloro pattern); HPLC Purity: 95.45%.

N-(1-(4-chlorobenzoyl)-1,2,3,4 tetrahydroquinolin-6-yl)-4-methylbenzamide (HB-UC-7) (9j):

The procedure remained same as that of the compound **9d**, only instead of 4-nitro benzoyl chloride; 4-methyl benzoyl chloride (1.6 mmol, 0.24 mL) was taken. Pale yellow Solid Yield: 57.14 %; mp: 209-211°C; IR (KBr, γ_{max} cm⁻¹): 841 (C-Cl), 1532 (C=O), 1671

(C=C), 2360 (C-N), 2938 (C-H aliphatic), 3037 (C-H aromatic), 3044 (-NH); ^1H NMR (400 MHz, DMSO- d_6) δ PPM: 1.96 (m, 2H, -CH₂), 2.37 (s, 1H, -CH₃), 2.80-2.83 (m, 2H, -CH₂), 3.73 (t, 2H, J = 6 Hz, -CH₂), 6.69 (s, 1H, Ar-CH), 7.25 (d, 1H, J = 8.4 Hz, Ar-CH), 7.31 (d, 2H, J = 8 Hz, Ar-CH), 7.34 (d, 2H, J = 8 Hz, Ar-CH), 7.41 (d, 2H, J = 8.4 Hz, Ar-CH), 7.71 (s, 1H, Ar-CH), 7.83 (d, 2H, J = 8 Hz, Ar-CH), 10.09 (s, 1H, NH-C=O); ^{13}C NMR (100 MHz, DMSO- d_6) δ PPM: 20.97, 23.52, 26.49, 44.20, 117.58, 119.97, 125.03, 127.58, 128.21, 128.86, 129.10 (2C), 129.30(2C), 130.10 (2C), 131.79 (2C), 135.37, 135.71, 141.50, 165.09, 167.89; MS (EI) m/z calculated for C₂₀H₁₉ClN₂O₄ 405 (M+1), found 422.0 (M+18 for water adduct) 423.9 (M+20 for Chloro Pattern); HPLC Purity: 96.01%.

N-(1-(4-chlorobenzoyl)-1,2,3,4-tetrahydroquinolin-6-yl)-3,5-bis(trifluoromethyl) benzamide (HB-UC-9) (9k):

The procedure remained same as that of the compound **9d**, only instead of 4-nitro benzoyl chloride; 3,5-bis(trifluoromethyl)benzoyl chloride (1.7 mmol, 0.31 mL) was taken. Pale yellow Solid Yield: 91.95 %; mp: 230-232°C; IR (KBr, γ_{max} cm⁻¹): 840 (C-Cl), 1545 (C=O), 1644 (C=C), 2360 (C-N), 2941 (C-H aliphatic), 3076 (C-H aromatic), 3292 (-NH); ^1H NMR (400 MHz, DMSO- d_6) δ PPM: 1.98 (m, 2H, -CH₂), 2.85 (m, 2H, -CH₂), 3.77 (m, 2H, -CH₂), 6.78 (s, 1H, Ar-CH), 7.28-7.38 (m, 4H, Ar-CH), 7.42 (m, 1H, Ar-CH), 7.70 (s, 1H, Ar-CH), 8.37-8.59 (d, 3H, Ar-CH), 10.59 (s, 1H, NH-C=O); ^{13}C NMR (100 MHz, DMSO- d_6) δ PPM: 23.45, 26.47, 40.07, 117.90, 120.35, 121.72, 124.43, 125.17(2C), 128.22(2C), 128.41, 130.08, 130.26, 130.59, 131.87, 134.52(2C), 134.82(2C), 134.90, 136.96(2C), 162.16, 167.99; MS (EI) m/z calculated for C₂₅H₁₇ClF₆N₂O₂ 527 (M+1), found 526.9 (M+1); HPLC Purity: 96.05 %.

N-(1-(4-chlorobenzoyl)-1,2,3,4-tetrahydroquinolin-6-yl)-4-fluorobenzamide (HB-UC-10) (9l):

The procedure remained same as that of the compound **9d**, only instead of 4-nitro benzoyl chloride; 4-fluoro benzoyl chloride (1.7 mmol, 0.2 mL) was taken. Pale yellow Solid Yield: 97.18 %; mp: 219-223°C; IR (KBr, γ_{max} cm⁻¹): 840 (C-Cl), 1545 (C=O), 1644 (C=C), 2360 (C-N), 2941 (C-H aliphatic), 3076 (C-H aromatic), 3292 (-NH); ^1H NMR (400 MHz, DMSO- d_6) δ PPM: 1.96 (m, 2H, -CH₂),

2.85 (m, 2H, -CH₂), 3.75 (m, 2H, -CH₂), 6.71 (s, 1H, Ar-CH), 7.25 (m, 1H, Ar-CH), 7.36-7.41 (m, 5H, Ar-CH), 7.70-8.01 (m, 3H, Ar-CH), 10.20 (s, 1H, NH-C=O); ¹³C NMR (100 MHz, DMSO-d₆) δ PPM: 23.51, 26.49, 44.22, 115.40, 117.64, 120.04, 125.08, 128.21, 128.43, 129.50, 130.10(2C), 130.22(2C), 131.23(2C), 131.82(2C), 134.37, 135.50, 162.77, 164.24, 167.92; MS (EI) m/z calculated for C₂₃H₁₈ClFN₂O₂ 409 (M+1), found 408.9 (M+1); HPLC Purity: 96.94 %.

N-(1-(4-chlorobenzoyl)-1,2,3,4-tetrahydroquinolin-6-yl)-4-methylbenzenesulfonamide (HB-UC-11) (9m)

The procedure remained same as that of the compound **9d**, only instead of 4-nitro benzoyl chloride; 4-methyl benzene sulfonyl chloride (3.4 mmol, 0.6 gm) was taken. Pale yellow Solid Yield: 88.19 %; mp: 240-242°C; IR (KBr, γ_{max} cm⁻¹): 821 (C-Cl), 1597 (C=O), 1643 (C=C), 2359 (C-N), 2927 (C-H aliphatic), 3059 (C-H aromatic), 3437 (-NH); ¹H NMR (400 MHz, DMSO-d₆) δ PPM: 2.29 (m, 2H, -CH₂), 2.82 (m, 2H, -CH₂), 3.75 (m, 2H, -CH₂), 7.12-7.14 (m, 2H, Ar-CH), 7.26-7.27 (m, 1H, Ar-CH), 7.34-7.51 (s, 1H, Ar-CH), 7.52-7.53 (m, 2H, Ar-CH), 7.56-7.58 (m, 2H, Ar-CH), 7.59-7.60 (m, 2H, Ar-CH), 7.70 (s, 1H, Ar-CH), 10.25 (s, 1H, NH-C=O); ¹³C NMR (100 MHz, DMSO-d₆) δ PPM: 23.32, 26.25, 40.05, 117.66, 120.07, 125.07, 126.68, 128.13, 128.23, 134.49 (2C), 135.33(2C), 135.40(2C), 136.04(2C), 136.34, 136.43, 137.89, 143.10, 145.23, 167.93; MS (EI) m/z calculated for C₂₃H₂₁ClN₂O₃S 441 (M+1), found 440.9 (M+1), 442 (for chloro pattern); HPLC Purity: 97.78%.

4-chloro-N-(1-(4-chlorobenzoyl)-1,2,3,4-tetrahydroquinolin-6-yl) benzenesulfonamide (HB-UC-13) (9n):

The procedure remained same as that of the compound **9d**, only instead of 4-nitro benzoyl chloride; 4-chloro benzene sulfonyl chloride (1.7 mmol, 0.36 gm) was taken. Dark yellow Solid Yield: 77.20 %; mp: 252-254°C; IR (KBr, γ_{max} cm⁻¹): 832 (C-Cl), 1534 (C=O), 1643 (C=C), 2360 (C-N), 2947 (C-H aliphatic), 3084 (C-H aromatic), 3338 (-NH); ¹H NMR (400 MHz, DMSO-d₆) δ PPM: 1.88 (m, 2H, -CH₂), 2.72 (m, 2H, -CH₂), 3.37-3.68 (m, 2H, -CH₂), 6.54-6.96 (m, 3H, Ar-CH), 7.26-7.35 (m, 2H, Ar-CH), 7.64-7.93 (m, 6H, Ar-CH), 10.21 (s, 1H, NH-C=O); ¹³C NMR (100 MHz, DMSO-d₆) δ PPM: 23.49, 26.24, 44.33, 118.04, 120.83, 125.67(2C), 128.10(2C), 128.23, 128.62, 129.29, 129.99(2C), 131.2(2C), 132.64, 133.39, 134.54, 135.02, 135.40, 137.79; MS (EI) m/z calculated for C₂₂H₁₈Cl₂N₂O₃S 461 (M+1); found 460.9 (M+1), 462.9 (for chloro pattern); HPLC Purity: 96.35%.

2-chloro-N-(1-(4-chlorobenzoyl)-1,2,3,4-tetrahydroquinolin-6-yl)acetamide (HB-UC-14) (9o):

The procedure remained same as that of the compound **9d**, only instead of 4-nitro benzoyl chloride; chloracetyl chloride (1.6 mmol, 0.13 mL) was taken. Dark yellow Solid Yield: 90.21 %; mp: 150-152°C; IR (KBr, γ_{max} cm⁻¹): 840 (C-Cl), 1545 (C=O), 1644 (C=C), 2360 (C-N), 2941 (C-H aliphatic), 3076 (C-H aromatic), 3292 (-NH); ¹H NMR (400 MHz, DMSO-d₆) δ PPM: 1.92-1.95 (m, 2H, -CH₂), 2.79 (m, 2H, -CH₂), 3.38-3.78 (m, 2H, -CH₂), 4.21 (s, 1H, -CH₂), 7.05-7.07 (m, 1H, Ar-CH), 7.33-7.35 (m, 1H, Ar-CH), 7.40 (s, 1H, Ar-CH), 7.42-7.48 (m, 2H, Ar-CH), 7.50-7.52 (m, 2H, Ar-CH), 10.24 (s, 1H, NH-C=O); ¹³C NMR (100 MHz, DMSO-d₆) δ PPM: 23.44, 26.43, 43.49, 44.29, 116.65, 119.04, 125.26, 128.21, 129.37(2C), 130.05(2C), 131.26, 132.11, 134.51, 135.27, 164.40, 167.92; MS (EI) m/z calculated for C₁₈H₁₆Cl₂N₂O₂ 363 (M+1), found 362.9 (M+1), 364.8 (for chloro pattern); HPLC Purity: 98.52 %.

Synthesis of Final Derivatives (Series-II):

Synthesis of N-(1-benzoyl-1,2,3,4-tetrahydroquinolin-6-yl)-4-nitrobenzamide (HB-UC-15) (10d):

Compound **8b** (1.9 mmol, 0.5 gm) was dissolved in the dichloromethane. Dropwise trimethylamine (3.8 mmol, 0.52 mL) was added to above reaction mixture and allowed to stir for 30 minutes at room temperature. 4-nitro benzoyl chloride (1.4 mmol, 0.36 gm) was added to above reaction mixture and stirring was continued for 1 hour. Reaction mixture was transferred to the crushed ice and extracted with dichloromethane dried over the sodium sulfate and passed through the column for the purification resulted into yellow colored compound. Dark yellow Solid Yield: 60.21 %; mp: 170-173°C; IR (KBr, γ_{max} cm⁻¹): 1545 (C=O), 1643 (C=C), 2360 (C-N), 2944 (C-H aliphatic), 3316 (C-H aromatic), 3316 (-NH); ¹H NMR (400 MHz, DMSO-d₆) δ PPM: 1.95 (m, 2H, -CH₂), 2.72 (m, 2H, -CH₂), 3.75 (m, 2H, -CH₂), 6.79 (s, 1H, Ar-CH), 7.04-7.36 (m, 4H, Ar-CH), 7.70 (s, 1H, Ar-CH), 8.16-8.36 (m, 6H, Ar-CH), 10.51 (s, 1H, NH-C=O); ¹³C NMR (100 MHz, DMSO-d₆) δ PPM: 23.50, 26.50, 44.48, 117.66, 120.15, 123.52, 125.06, 128.02, 128.16(2C), 129.09 (3C), 129.89 (2C), 131.57(2C), 134.96, 136.54, 140.50, 149.06, 163.56, 169.13; MS (EI) m/z calculated for C₂₃H₁₉N₃O₄ 402 (M+1), found 402 (M+1); HPLC Purity : 95.87 %.

Synthesis of N-(1-benzoyl-1,2,3,4-tetrahydroquinolin-6-yl)-4-chlorobenzamide (HB-UC-16) (10e):

The procedure remained same as that of the compound **10d**, only instead of 4-nitro benzoyl chloride; 4-chloro benzoyl chloride (1.9 mmol, 0.26 mL) was taken. Pale yellow Solid Yield: 50.14 %; mp: 175-178°C; IR (KBr, γ_{\max} cm^{-1}): 1534 (C=O), 1627 (C=C), 2359 (C-N), 2949 (C-H aliphatic), 3063 (C-H aromatic), 3355 (-NH); ^1H NMR (400 MHz, DMSO- d_6) δ PPM: 1.94 (m, 2H, CH_2), 2.80 (t, J = 4 Hz, 2H, $-\text{CH}_2$), 3.78 (m, 2H, $-\text{CH}_2$), 6.71 (s, 1H, Ar-CH), 7.57 (d, J = 8 Hz, 1H, Ar-CH), 7.34(d, J = 8 Hz, 2H, Ar-CH), 7.40 (d, J = 8 Hz, 2H, Ar-CH), 7.51 (m, 1H, Ar-CH), 7.55 (t, J = 8 Hz, 2H, Ar-CH), 7.76 (s, 1H, Ar-CH), 7.92 (d, J = 8 Hz, 2H, Ar-CH), 10.11(s, 1H, NH-C=O); ^{13}C NMR (100 MHz, DMSO- d_6) δ PPM: 23.42, 26.10, 44.53, 117.12, 128.11, 120.05, 125.19, 134.31, 127.16, 136.41, 129.11(2C), 135.21(2C), 134.11, 135.55, 128.13(2C), 130.19(2C), 135.46, 165.11, 167.89; MS (EI) m/z calculated for $\text{C}_{23}\text{H}_{19}\text{ClN}_2\text{O}_2$ 391 (M+1), found 391 (M+1); HPLC Purity: 98.13 %.

Synthesis of N-(1-benzoyl-1,2,3,4-tetrahydroquinolin-6-yl)-4-bromobenzamide (HB-UC-17) (10f):

The procedure remained same as that of the compound **10d**, only instead of 4-nitro benzoyl chloride; 4-bromo benzoyl chloride (1.9 mmol, 0.43 gm) was taken. Pale yellow Solid Yield: 45.10 %; mp: 173-175°C; IR (KBr, γ_{\max} cm^{-1}): 1532 (C=O), 1644 (C=C), 2360 (C-N), 2931(C-H aliphatic), 3061 (C-H aromatic), 3314 (-NH); ^1H NMR (400 MHz, DMSO- d_6) δ PPM: 1.96 (m, 2H, $-\text{CH}_2$), 2.82 (m, 2H, $-\text{CH}_2$), 3.75 (m, 2H, $-\text{CH}_2$), 6.77 (m, 2H, Ar-CH), 7.36 (s, 1H, Ar-CH), 7.72-7.88 (m, 9H, Ar-CH), 10.25 (s, 1H, NH-C=O); ^{13}C NMR (100 MHz, DMSO- d_6) δ PPM: 23.19, 26.50, 67.34, 117.59, 120.06, 125.00, 128.63, 129.49, 129.86(2C), 131.26(2C), 131.35, 131.57(2C), 132.27(2C), 133.87, 134.69, 135.18, 136.57, 164.02, 164.25; MS (EI) m/z calculated for $\text{C}_{23}\text{H}_{18}\text{BrN}_3\text{O}_4$ 436.4 (M+1), found 436.4 (M+1), 438.4 (for bromo pattern); HPLC Purity: 98.04 %.

Synthesis of N-(1-benzoyl-1,2,3,4-tetrahydroquinolin-6-yl)benzamide (HB-UC-18) (10g):

The procedure remained same as that of the compound **10d**, only instead of 4-nitro benzoyl chloride; benzoyl chloride (1.9 mmol, 0.22 mL) was taken. White Solid Yield: 80.10 %; mp: 165-168°C; IR (KBr, γ_{\max} cm^{-1}): 1597 (C=O), 1672 (C=C), 2360 (C-N), 2945 (C-H aliphatic), 3032 (C-H aromatic), 3325 (-NH); ^1H NMR (400 MHz, DMSO- d_6) δ PPM: 1.96 (m, 2H, $-\text{CH}_2$), 2.82 (m, 2H, $-\text{CH}_2$), 3.75 (m, 2H, $-\text{CH}_2$), 6.74 (m, 1H, Ar-CH), 7.24 (d, 4H, J = 7.2 Hz, Ar-CH), 7.35 (m, 2H, Ar-CH), 7.51 (m, 2H, Ar-CH), 7.56 (m, 2H, Ar-CH),

7.70 (s, 1H, Ar-CH), 7.91 (d, 1H, J = 6.4 Hz, Ar-CH), 10.25 (s, 1H, NH-C=O); ^{13}C NMR (100 MHz, DMSO- d_6) δ PPM: 23.55, 26.52, 44.38, 117.55, 120, 124.97, 126.95(2C), 127.54(2C), 128.03, 128.13(2C), 128.33(2C), 129.84, 131.47, 134.55, 134.88, 135.43, 136.61, 165.28, 169.07 MS (EI) m/z calculated for $\text{C}_{23}\text{H}_{20}\text{N}_2\text{O}_2$ 357.1 (M+1), found 357.1 (M+1), 374 (M+18 for water adduct); HPLC Purity: 97.92%.

Synthesis of 4-amino-N-(1-benzoyl-1,2,3,4-tetrahydroquinolin-6-yl)benzamide (HB-UC-19) (10h):

The procedure remained same as that of the compound **9h**, only instead of compound **9d**, compound **10d** (1.2 mmol, 0.5 gm) was used with 10 equivalent zinc and 7 equivalent ammonium chloride for the reduction. Dark yellow Solid Yield: 84.17 %; mp: 160-163°C; IR (KBr, γ_{max} cm^{-1}): 1508 (C=O), 1641 (C=C), 2360 (C-N), 2931 (C-H aliphatic), 3054 (C-H aromatic), 3348 (-NH); ^1H NMR (400 MHz, DMSO- d_6) δ PPM: 1.95 (m, 2H, -CH $_2$), 2.80 (m, 2H, -CH $_2$), 3.74 (m, 2H, -CH $_2$), 5.75 (s, 2H, -NH), 6.59 (m, 3H, Ar-CH), 7.34 (m, 5H, Ar-CH), 7.68 (m, 4H, Ar-CH), 9.67 (s, 1H, NH-C=O); ^{13}C NMR (100 MHz, DMSO- d_6) δ PPM: 23.58, 26.52, 44.27, 112.50, 117.29, 119.68, 120.98, 124.86, 128.01, 128.11(2C), 129.23(2C), 129.79(2C), 131.32(2C), 133.88, 136.10, 136.67, 152.07, 165.06, 168.98; MS (EI) m/z calculated for 372 (M+1), $\text{C}_{23}\text{H}_{21}\text{N}_3\text{O}_2$, found 372 (M+1); HPLC Purity: 96.19%.

Ethyl 2-(1-benzoyl-1,2,3,4-tetrahydroquinolin-6-ylamino)-2-oxoacetate (HB-UC-20) (10i):

The procedure remain same as that of the compound **10d**, only instead of 4-nitro benzoyl chloride; ethyl 2-chloro-2-oxoacetate (1.9 mmol, 0.22 mL) was used. Pale yellow Solid Yield: 79.19 %; mp: 140-142°C; IR (KBr, γ_{max} cm^{-1}): 1532 (C=O), 1643 (C=C), 2360 (C-N), 2939 (C-H aliphatic), 3072 (C-H aromatic), 3344 (-NH); ^1H NMR (400 MHz, DMSO- d_6) δ PPM: 1.30 (m, 3H, -CH $_3$), 1.93 (m, 2H, -CH $_2$), 2.80 (m, 2H, -CH $_2$), 3.73 (m, 2H, -CH $_2$), 4.29 (m, 2H, -CH $_2$), 6.78 (s, 1H, Ar-CH), 7.24-7.35 (m, 6H, Ar-CH), 7.65 (s, 1H, Ar-CH), 10.69 (s, 1H, NH-C=O); ^{13}C NMR (100 MHz, DMSO- d_6) δ PPM: 13.80, 23.42, 26.47, 44.45, 62.32, 117.65, 120.09, 125.07, 128.01, 128.14, 129.91, 131.56, 133.66 (2C), 135.46 (2C), 136.47, 155.26, 160.60, 169.16; MS (EI) m/z calculated for $\text{C}_{20}\text{H}_{20}\text{N}_2\text{O}_4$ 353 (M+1), found 353.1 (M+1); HPLC Purity: 98.44%.

N-(1-benzoyl-1,2,3,4-tetrahydroquinolin-6-yl)-4-methylbenzamide (HB-UC-21) (10j):

The procedure remain same as that of the compound **10d**, only instead of 4-nitro benzoyl chloride; 4-methyl benzoyl chloride (1.9 mmol, 0.25 mL) was used. Pale yellow Solid Yield: 69.29 %; mp: 169-171°C; IR (KBr, γ_{\max} cm^{-1}): 1517 (C=O), 1656 (C=C), 2359 (C-N), 2927 (C-H aliphatic), 3056 (C-H aromatic), 3339 (-NH); ^1H NMR (400 MHz, DMSO- d_6) δ PPM: 1.94-1.99 (m, 3H, -CH₂), 2.37 (s, 3H, -CH₃), 2.80-2.83 (m, 2H, -CH₂), 3.73-3.76 (m, 2H, -CH₂), 7.25 (d, 2H, J = 8 Hz, Ar-CH), 7.30 (d, 2H, J = 8 Hz, Ar-CH), 7.32-7.34 (m, 1H, Ar-CH), 7.35 (d, 2H, J = 8 Hz, Ar-CH), 7.38 (d, 2H, J = 8 Hz, Ar-CH), 7.39-7.41 (m, 1H, Ar-CH), 7.70 (s, 1H, Ar-CH), 7.84-7.86 (m, 1H, Ar-CH), 10.10 (s, 1H, NH-C=O); ^{13}C NMR (100 MHz, DMSO- d_6) δ PPM: 20.97, 23.55, 26.51, 44.36, 124.93, 127.59, 128.02, 128.13, 128.85, 129.30, 129.83 (2C), 130.38, 131.43(2C), 131.94(2C), 134.43(2C), 135.52, 136.61, 141.47, 165.08, 169.04; MS (EI) m/z calculated for C₂₄H₂₂N₂O₂ 371 (M+1), found 371.1 (M+1); HPLC Purity: 97.33%.

N-(1-benzoyl-1,2,3,4-tetrahydroquinolin-6-yl)-3,5-bis(trifluoromethyl)benzamide (HB-UC-23) (10k):

The procedure remain same as that of the compound **10d**, only instead of 4-nitro benzoyl chloride; 3,5-bis(trifluoromethyl)benzoyl chloride (1.9 mmol, 0.35 mL) was used. Pale yellow Solid Yield: 64.10 %; mp: 198-200°C; IR (KBr, γ_{\max} cm^{-1}): 1136 (C-F), 1547 (C=O), 1644 (C=C), 2360 (C-N), 2943 (C-H aliphatic), 3071 (C-H aromatic), 3302 (-NH); ^1H NMR (400 MHz, DMSO- d_6) δ PPM: 1.96-1.99 (m, 2H, -CH₂), 2.83-2.87 (m, 2H, -CH₂), 3.75-3.78 (m, 2H, -CH₂), 6.82 (s, 1H, Ar-CH), 7.26 (d, 2H, J = 8.4 Hz, Ar-CH), 7.36-7.37 (m, 1H, Ar-CH), 7.40 (t, 2H, J = 4.4 Hz, Ar-CH), 7.54 (d, 2H, J = 8 Hz, Ar-CH), 7.68 (s, 1H, Ar-CH), 8.40 (s, 1H, Ar-CH), 8.59 (s, 1H, Ar-CH), 10.57 (s, 1H, NH-C=O); ^{13}C NMR (100 MHz, DMSO- d_6) δ PPM: 23.47, 26.48, 44.45, 117.81, 119, 120.34, 121.72 (2C), 124.43(2C), 125.07(2C), 127.14 (2C), 128.01, 129.87, 130.27, 130.58, 130.91, 131.53, 134.63, 135.12, 136.53, 162.14, 169.13; MS (EI) m/z calculated for C₂₅H₁₈F₆N₂O₂ 493 (M+1), found 492.9 (M+1); HPLC Purity: 97.35%.

N-(1-benzoyl-1,2,3,4-tetrahydroquinolin-6-yl)-4-fluorobenzamide (HB-UC-24) (10l):

The procedure remain same as that of the compound **10d**, only instead of 4-nitro benzoyl chloride; 4-fluoro benzoyl chloride (1.9 mmol, 0.23 mL) was used. Pale yellow Solid Yield: 59.20 %; mp: 180-182°C; IR (KBr, γ_{\max} cm^{-1}): 1599 (C=O), 1671 (C=C), 2359 (C-N), 2956 (C-H aliphatic), 3070 (C-H aromatic), 3352 (-NH); ^1H NMR (400 MHz, DMSO- d_6) δ PPM: 1.94-1.97 (m, 2H, -CH₂), 2.81-2.84

(m, 2H, -CH₂), 3.74 (m, 2H, -CH₂), 6.76 (s, 1H, Ar-CH), 7.24 (m, 1H, Ar-CH), 7.26 (d, 2H, J = 8 Hz, Ar-CH), 7.36-7.47 (m, 4H, Ar-CH), 7.69 (s, 1H, Ar-CH), 7.99-8.01 (m, 1H, Ar-CH), 8.01 (d, 2H, J = 6 Hz, Ar-CH), 10.18 (s, 1H, NH-C=O); ¹³C NMR (100 MHz, DMSO-d₆) δ PPM: 23.53, 26.50, 44.38, 115.38, 120.05, 124.98, 128.02(2C), 128.13 (2C), 129.84 (2C), 130.21(2C), 131.25, 131.28, 133.53, 133.63, 134.61, 135.31, 136.60, 165.23, 169.06 MS (EI) m/z calculated for C₂₃H₁₉FN₂O₂ 375 (M+1); found 375 (M+1); HPLC Purity: 98.41 %.

N-(1-benzoyl-1,2,3,4-tetrahydroquinolin-6-yl)-4-chlorobenzenesulfonamide (HB-UC-25) (10n):

The procedure remain same as that of the compound **10d**, only instead of 4-nitro benzoyl chloride; 4-chloro benzene sulfonyl chloride (3.9 mmol, 0.8 gm) was used. Pale yellow Solid Yield: 80.20 %; mp: 180-183°C; IR (KBr, γ_{max} cm⁻¹): 1502 (C=O), 1622 (C=C), 2360 (C-N), 2913 (C-H aliphatic), 3060 (C-H aromatic), 3372 (-NH); ¹H NMR (400 MHz, DMSO-d₆) δ PPM: 1.84-1.87 (m, 2H, -CH₂), 2.70-2.71 (m, 2H, -CH₂), 3.67 (m, 2H, -CH₂), 6.57 (d, 1H, J = 6.8 Hz, Ar-CH), 6.69 (s, 1H, Ar-CH), 6.94 (s, 1H, Ar-CH), 7.27 (m, 1H, Ar-CH), 7.29 (t, 2H, J = 7.2 Hz, Ar-CH), 7.38 (d, 2H, J = 6.8 Hz, Ar-CH), 7.62 (d, 2H, J = 8.4 Hz, Ar-CH), 7.69 (d, 2H, J = 8 Hz, Ar-CH), 10.23 (s, 1H, NH-C=O); ¹³C NMR (100 MHz, DMSO-d₆) δ PPM: 23.29, 26.26, 44.47, 117.89, 120.59(2C), 125.60 (2C), 126.95, 127.90 (2C), 128.05 (2C), 129.34, 129.82, 132.17, 133.30, 135.49, 136.33, 137.71, 138.07, 169.12; MS (EI) m/z calculated for C₂₂H₁₉ClN₂O₃S 427 (M+1), found 426.9 (M+1), 428.8 (for chloro pattern); HPLC Purity: 97.42 %.

Synthesis of Final Derivatives (Series-III):

N-(1-(2-ethylbutanoyl)-1,2,3,4-tetrahydroquinolin-6-yl)-4-nitrobenzamide (HB-UC-31) (11d):

Compound **8c** (2 mmol, 0.5 gm) was dissolved in the dichloromethane. Dropwise trimethylamine (4 mmol, 0.56 mL) was added to above reaction mixture and allowed to stir for 30 minutes at room temperature. 4-nitro benzoyl chloride (1.5 mmol, 0.37 gm) was added to above reaction mixture and stirring was continued for 1 hour. Reaction mixture was transferred to the crushed ice and extracted with dichloromethane dried over the sodium sulfate and passed through the column for the purification resulted into yellow colored compound. Orange Sticky Solid Yield: 69.10 %; mp: 165-169°C; IR (KBr, γ_{max} cm⁻¹): 1530 (C=O), 1673 (C=C), 2360 (C-N), 2961

(C-H aliphatic), 3071 (C-H aromatic), 3400 (-NH); ^1H NMR (400 MHz, DMSO- d_6) δ PPM: 0.78 (m, 6H, -CH₃), 1.23-1.40 (m, 4H, -CH₂), 1.89 (m, 2H, -CH₂), 2.81 (m, 2H, -CH₂), 3.37 (m, 1H, -CH), 3.71 (m, 2H, -CH₂), 7.15-7.69 (m, 3H, Ar-CH), 8.20-8.38 (m, 4H, Ar-CH), 10.60 (s, 1H, NH-C=O); ^{13}C NMR (100 MHz, DMSO- d_6) δ PPM: 11.60(2C), 23.82(2C), 25.23, 26.31, 41.97, 43.74, 118.85, 120.16, 123.54, 125.05(2C), 128.22, 129.06(2C), 129.13(2C), 140.51, 149.08, 163.68, 174.77; MS (EI) m/z calculated for C₂₂H₂₅N₃O₄ 396 (M+1), found 396.1 (M+1); HPLC Purity: 96.01%.

4-chloro-N-(1-(2-ethylbutanoyl)-1,2,3,4-tetrahydroquinolin-6-yl)benzamide (HB-UC-32) (11e):

The procedure remain same as that of the compound **11d**, only instead of 4-nitro benzoyl chloride; 4-chloro benzoyl chloride (2 mmol, 0.26 mL) was used. Orange Sticky Solid Yield: 59.45 %; mp: 169-171°C; IR (KBr, γ_{max} cm⁻¹): 1532 (C=O), 1645 (C=C), 2359 (C-N), 2962 (C-H aliphatic), 3063 (C-H aromatic), 3313 (-NH); ^1H NMR (400 MHz, DMSO- d_6) δ PPM: 0.77 (m, 6H, -CH₃), 1.23 (m, 4H, -CH₂), 1.90 (m, 2H, -CH₂), 2.80 (m, 2H, -CH₂), 3.35 (m, 1H, -CH), 3.70 (m, 2H, -CH₂), 7.25 (m, 2H, Ar-CH), 7.69 (s, 1H, Ar-CH), 8.13 (m, 2H, Ar-CH), 8.17 (m, 2H, Ar-CH), 10.10 (s, 1H, NH-C=O) ^{13}C NMR (100 MHz, DMSO- d_6) δ PPM: 11.10(2C), 23.22(2C), 25.13, 26.41, 41.95, 43.75, 118.83, 120.19, 123.14, 125.19(2C), 128.42 (2C), 129.04, 129.23(2C), 140.11, 149.18, 163.58, 174.17; MS (EI) m/z calculated for C₂₂H₂₅ClN₂O₂ 385 (M+1), found 385.1 (M+1) and 387.1 (M+2) for chloro pattern; HPLC Purity: 95.41%.

4-bromo-N-(1-(2-ethylbutanoyl)-1,2,3,4-tetrahydroquinolin-6-yl)benzamide (HB-UC-33) (11f)

The procedure remain same as that of the compound **11d**, only instead of 4-nitro benzoyl chloride; 4-bromo benzoyl chloride (2 mmol, 0.4 gm) was used. Orange Sticky Solid Yield: 60.40 %; mp: 175-178°C; IR (KBr, γ_{max} cm⁻¹): 1499 (C=O), 1641 (C=C), 2355 (C-N), 2955 (C-H aliphatic), 3065 (C-H aromatic), 3304 (-NH); ^1H NMR (400 MHz, DMSO- d_6) δ PPM: 0.81 (m, 6H, -CH₃), 1.22-1.40 (m, 2H, -CH₂), 1.89 (m, 2H, -CH₂), 2.80 (m, 2H, -CH₂), 2.66-2.81 (m, 2H, -CH₂), 3.36 (m, 1H, CH), 3.71-3.76 (m, 2H, -CH₂), 7.76-7.90 (m, 3H, Ar-CH), 8.02-8.09 (m, 4H, Ar-CH), 10.27 (s, 1H, NH-C=O); ^{13}C NMR (100 MHz, DMSO- d_6) δ PPM: 11.60 (2C), 23.81(2C), 25.23, 26.31, 43.74, 44.19, 120.09, 125.02, 125.30, 129.72, 130.12, 131.26(2C), 131.38(2C), 131.66, 133.90, 135.80, 164.38, 174.25; MS (EI) m/z calculated for C₂₂H₂₅BrN₂O₂ 429 (M+1), found 429 (M+1), 431 (for bromo pattern); HPLC Purity: 96.15%.

N-(1-(2-ethylbutanoyl)-1,2,3,4-tetrahydroquinolin-6-yl)benzamide (HB-UC-34) (11g):

The procedure remain same as that of the compound **11d**, only instead of 4-nitro benzoyl chloride; simple benzoyl chloride (2 mmol, 0.2 mL) was used. Orange Sticky Solid Yield: 78.15 %; mp: 171-173°C; IR (KBr, γ_{\max} cm⁻¹): 1536 (C=O), 1645 (C=C), 2359 (C-N), 2961 (C-H aliphatic), 3060 (C-H aromatic), 3313 (-NH); ¹H NMR (400 MHz, DMSO-d₆) δ PPM: 0.76 (m, 6H, -CH₃), 1.23 (m, 4H, -CH₂), 1.88 (m, 2H, -CH₂), 2.80 (m, 2H, -CH₂), 3.51 (m, 1H, -CH), 3.70 (m, 2H, -CH₂), 7.55-7.59 (m, 3H, Ar-CH), 7.96-8.04 (m, 5H, Ar-CH), 10.50 (s, 1H, NH-C=O); ¹³C NMR (100 MHz, DMSO-d₆) δ PPM: 11.63(2C), 23.81(2C), 24.13, 25.31, 42.70, 45.20, 117.45, 120.10, 123.44, 125.15(2C), 128.29, 129.16, 130.12(3C), 140.31, 149.18, 162.09, 174.87 MS (EI) m/z calculated for C₂₂H₂₆N₂O₂ 351 (M+1); found 368.2 (M+18); HPLC Purity: 97.09%.

N-(1-(2-ethylbutanoyl)-1,2,3,4-tetrahydroquinolin-6-yl)-4-methylbenzamide (HB-UC-36) (11j):

The procedure remain same as that of the compound **11d**, only instead of 4-nitro benzoyl chloride; 4-methyl benzoyl chloride (2 mmol, 0.26 mL) was used. Orange Sticky Solid Yield: 86.15 %; mp: 170-175°C; IR (KBr, γ_{\max} cm⁻¹): 1534 (C=O), 1650 (C=C), 2359 (C-N), 2961 (C-H aliphatic), 3036 (C-H aromatic), 3312 (-NH); ¹H NMR (400 MHz, DMSO-d₆) δ PPM: 0.76 (m, 6H, -CH₃), 1.22-1.39 (m, 4H, -CH₂), 1.88 (m, 2H, -CH₂), 2.38 (s, 3H, -CH₃), 2.65-2.80 (m, 2H, -CH₂), 3.36 (m, 1H, -CH), 3.70 (m, 2H, -CH₂), 7.08-7.15 (m, 3H, Ar-CH), 7.25-7.33 (m, 1H, Ar-CH), 7.68-7.86 (m, 3H, Ar-CH), 10.29 (s, 1H, NH-C=O); ¹³C NMR (100 MHz, DMSO-d₆) δ PPM: 11.61 (2C), 20.98, 21.09 (2C), 23.84, 25.24, 26.31, 40.69, 43.70, 118.11, 120.01, 124.92 (2C), 127.61, 128.22 (2C), 128.88, 129.30, 131.98, 141.52, 165.19, 174.74; MS (EI) m/z calculated for C₂₃H₂₈N₂O₂ 365 (M+1), found 365.2 (M+1); HPLC Purity: 96.58%.

N-(1-(2-ethylbutanoyl)-1, 2, 3, 4-tetrahydroquinolin-6-yl)-3, 5-bis (trifluoromethyl) benzamide (HB-UC-37) (11k):

The procedure remain same as that of the compound **11d**, only instead of 4-nitro benzoyl chloride; 3,5-bis(trifluoromethyl)benzoyl chloride (2 mmol, 0.36 mL) was used. Orange Sticky Solid Yield: 60.40 %; mp: 187-189°C; IR (KBr, γ_{\max} cm⁻¹): 1406 (C-F), 1530 (C=O), 1673 (C=C), 2360 (C-N), 2961 (C-H aliphatic), 3071 (C-H aromatic), 3400 (-NH); ¹H NMR (400 MHz, DMSO-d₆) δ PPM: 0.81 (m, 6H, -CH₃), 1.40-1.57 (m, 4H, -CH₂), 1.90 (m, 2H, -CH₂), 2.68-2.82 (m, 2H, -CH₂), 3.37 (m, 1H, -CH), 3.74 (m, 2H, -CH₂),

7.66-7.81 (m, 1H, Ar-CH), 7.89 (s, 1H, Ar-CH), 8.09 (s, 1H, Ar-CH), 8.45 (s, 2H, Ar-CH) 8.62 (s, 1H, Ar-CH), 10.68 (s, 1H, NH-C=O); ^{13}C NMR (100 MHz, DMSO- d_6) δ PPM: 10.05 (2C), 19.3, 25.14(2C), 28.80, 42.03, 46.85, 119.30, 120.42, 121.31, 124.06 (2C), 126.13, 127.96(2C), 131.21(2C), 131.65(2C), 133.50, 134.30, 163.19, 174.25; MS (EI) m/z calculated for $\text{C}_{24}\text{H}_{24}\text{F}_6\text{N}_2\text{O}_2$ 487 (M+1); found 487 (M+1); HPLC Purity: 95.17%.

N-(1-(2-ethylbutanoyl)-1,2,3,4-tetrahydroquinolin-6-yl)-4-fluorobenzamide (HB-UC-38) (11f):

The procedure remain same as that of the compound **11d**, only instead of 4-nitro benzoyl chloride; 4-fluoro benzoyl chloride (1000 mmol, 0.23 mL) was used. Orange Sticky Solid Yield: 58.19 %; mp: 166-169°C; IR (KBr, γ_{max} cm^{-1}): 1512 (C=O), 1620 (C=C), 2360 (C-N), 2912 (C-H aliphatic), 3050 (C-H aromatic), 3322 (-NH); ^1H NMR (400 MHz, DMSO- d_6) δ PPM: 0.78 (m, 6H, -CH₃), 1.23-1.54 (m, 4H, -CH₂), 1.88 (m, 2H, -CH₂), 2.51-2.81 (m, 2H, -CH₂), 3.37 (m, 1H, -CH), 3.71 (m, 2H, -CH₂), 7.38-7.78 (m, 3H, Ar-CH), 7.67-8.03 (m, 4H, Ar-CH), 10.29 (s, 1H, NH-C=O); ^{13}C NMR (100 MHz, DMSO- d_6) δ PPM: 11.60 (2C), 23.80, 25.23(2C), 26.30, 40.08, 43.75, 115.20, 115.42, 119.31, 120.06, 121.13, 124.96(2C), 129.21, 130.26(2C), 130.35, 131.30, 163.15, 174.75; MS (EI) m/z calculated for $\text{C}_{22}\text{H}_{25}\text{FN}_2\text{O}_2$ 369 (M+1); found 369.1 (M+1); HPLC Purity: 96.23%.

Ethyl 2-(1-(2-ethylbutanoyl)-1,2,3,4-tetrahydroquinolin-6-ylamino)-2-oxoacetate (HB-UC-39) (11i):

The procedure remain same as that of the compound **11d**, only instead of 4-nitro benzoyl chloride; simple ethyl 2-chloro-2-oxoacetate (2 mmol, 0.22 mL) was used. Orange Sticky Solid Yield: 84.10 %; mp: 150-152°C; IR (KBr, γ_{max} cm^{-1}): 1545 (C=O), 1657 (C=C), 2360 (C-N), 2965 (C-H aliphatic), 3074 (C-H aromatic), 3299 (-NH); ^1H NMR (400 MHz, DMSO- d_6) δ PPM: 0.75 (m, 6H, -CH₃), 1.31 (m, 4H, -CH₂), 1.51 (m, 3H, -CH₃), 2.63 (m, 2H, -CH₂), 2.77 (m, 2H, -CH₂), 3.68 (m, 2H, -CH₂), 4.28 (m, 1H, -CH), 4.30 (m, 2H, -CH₂), 7.10 (s, 1H, Ar-CH), 7.63 (s, 1H, Ar-CH), 8.07 (s, 1H, Ar-CH), 10.81 (s, 1H, NH-C=O); ^{13}C NMR (100 MHz, DMSO- d_6) δ PPM: 11.55 (2C), 13.80, 23.75, 25.22 (2C), 26.30, 41.92, 43.73, 62.35, 118.16, 120.15, 125.07, 125.38, 134.55, 135.62, 155.31, 160.63, 174.75; MS (EI) m/z calculated for $\text{C}_{19}\text{H}_{26}\text{N}_2\text{O}_4$ 347 (M+1), found 347.2 (M+1); HPLC Purity: 96.07 %.

2-chloro-N-(1-(2-ethylbutanoyl)-1,2,3,4-tetrahydroquinolin-6-yl)acetamide (HB-UC-41) (11o)

The procedure remain same as that of the compound **11d**, only instead of 4-nitro benzoyl chloride; chloracetyl chloride (2 mmol, 0.15 mL) was used. Orange Sticky Solid Yield: 70.43 %; mp: 138-140°C; IR (KBr, γ_{max} cm⁻¹): 1498 (C=O), 1646 (C=C), 2360 (C-N), 2927 (C-H aliphatic), 3283 (-NH); ¹H NMR (400 MHz, DMSO-d₆) δ PPM: 0.75-0.81 (m, 6H, -CH₃), 1.46-1.56 (m, 4H, -CH₂), 1.87-1.93 (m, 2H, -CH₃), 2.71-2.83 (m, 2H, -CH₂), 3.68-3.77 (m, 2H, -CH₂), 3.88 (m, 1H, -CH₂), 4.23 (m, 2H, -CH₂), 7.09-7.34 (m, 1H, Ar-CH), 7.47-7.59 (m, 1H, Ar-CH), 7.79 (s, 1H, Ar-CH), 10.44 (s, 1H, NH-C=O); ¹³C NMR (100 MHz, DMSO-d₆) δ PPM: 11.10 (2C), 18.20, 23.20(2C), 27.90, 40.10, 41.20, 45.30, 119.20, 120.40, 120.90, 129.10, 133.30, 134.20, 163.24, 174.50; MS (EI) m/z calculated for C₁₇H₂₃ClN₂O₂ 323 (M+1), found 323.1 (M+1); HPLC Purity: 95.24%.

mTOR Enzyme Assay

The Human Mammalian Target of Rapamycin (mTOR) ELISA kit was purchased from the Puregene (Cat. No. PG-3963H). Lung Cancer cell line (A549) was grown in the F-12 Ham's media supplemented with 5% Fatal Bovine Serum (FBS) and 0.5% pen-strep (Penicilline + Streptomycine). Cells were seeded in the wells as per the requirement followed by the treatment with the all 31 compounds along with the standards. Further, cell lysate was prepared with the aid of lysis buffer. This cell lysate was immediately taken for the analysis and further procedure was carried out as per ELISA kit user manual.

***In-Vitro* Antiproliferative MTT Assay**

All the synthesized Tetrahydroquinoline derivatives were screened through the panel of different human cancer cell lines viz. Lung cancer (A-549), Stomach Cancer (AGS), Colon Cancer (HCT-15), Skin Cancer (B16F1) for the evaluation of the antiprolifertive activity. In addition to that, these compounds were tested against the VERO cell line for the toxicity prediction. A VERO cell line is usually obtained from the kidney of an adult green monkey and is useful for the detection of the VERO toxin. Hence in the present research, we used this cell line for determining the toxicity of the synthesized compounds. The colon cancer (HCT-15) and the VERO cell lines were cultured in the RPMI-1650. The stomach cancer (AGS) and lung cancer (A549) cell lines were cultured in F-12 Ham's media. Skin Cancer (B16F1) cell line was cultured in DMEM. The entire media was made with the help of 5% Fatal Bovine Serum (FBS) as it provides nutrition to the cell line. Additionally, 0.5% pen-strep (Penicilline + Streptomycine) added to all the media in order to prevent

the cell line from contamination. All these cell lines were grown in a sterile vented T-75 flask placed in the incubator having a supply of 5% CO₂ along with the 37°C temperature. Stock solutions of all the compounds were made in the DMSO and dilutions were carried out in the respective media in such way that the final concentration of DMSO in the 96 well plates was not more than 0.1%. Initially, all the compounds were screened against all the cell lines in triplicate at a concentration of 25 µM. The compounds showing more than 50 % inhibition were taken for the preparation of the serial dilutions and IC₅₀ values were determined. 1×10⁴ cells were seeded on day 1 followed by the addition of the compounds after 24 hours. Compounds were incubated with the cells for 48 hours followed by the addition of the MTT dye. The MTT dye was kept for 4 hours and later removed from the wells. To dissolve the formazan crystals which were formed due to the live cells, 200 µL DMSO was added to each well and absorbance was taken at 570 nm.

Colony Forming Assay

A549 lung cancer cells were seeded in the 6 well plates with the density of 1000 cells per well. All the cells were supplemented with RPMI-1650, 5% CO₂, 5% FBS, and 0.5% pen-strep (Penicilline + Streptomycine). Cells were allowed to adhere and grow for 24 hours in 6 well plates. After 24 hours, the media was removed from each well and the compounds HB-UC-1, HB-UC-3, HB-UC-4, HB-UC-5, HB-UC-6 and HB-UC-9 were added separately at three different concentrations of 6.25 µM, 12.5 µM and 25 µM. The media was changed every third day and experiments were conducted up to 12 days. At the end of the twelfth day, the colonies were fixed with 4% paraformaldehyde and stained with 0.5% crystal violet solution. The images of all the colonies were taken and counting of colonies was done with the help of image J software. Microscopic images of colonies were taken with the help of an inverted microscope (400X). These experiments were performed in the duplicate and Mean ± SEM was calculated by applying one-way ANOVA (and nonparametric) with the help of post hoc Tukey's tests and Graph Pad Prism 5.

Cell Apoptosis Assay

A549 cells of lung cancer cell line were seeded in 6 well plates which were supplemented with F-12 Ham's media, 5% CO₂, 5% FBS, and 0.5% pen-strep (Penicilline + Streptomycine) at 37 °C for 24 hours. Later, the compounds HB-UC-1 and HB-UC-5 were added in two concentrations 3 µM and 6 µM, respectively. Two wells among the six wells were kept for the DMSO control and standard drug Everolimus. These treated and DMSO control cells were incubated for 48 hours. After the completion of the 48 hours, the media was removed from each well and 1 mL trypsin was added to each well for a minute followed by 4 mL media for neutralizing the effect of trypsin. Further all the procedure followed as per the user guideline of Annexin V-FITC apoptosis detection kit (Catalogue Number: APOAF). All the contents from each well were removed and transferred to the centrifuge tube. Centrifugation was carried out for 1000 RPM for 11 minutes. Media from each well was removed and pellets of the cells were washed with the PBS. Centrifugation was carried out again followed by the addition of the 1 mL binding buffer provided in the kit of the Annexin V-FITC apoptosis detection kit. These tubes were kept in the dark for 15 to 20 minutes. 500 µL of this cell suspension of the binding buffer was transferred to each plastic flow cytometric tubes. 5 µL Annexin-V FITC conjugate and 10 µL propidium iodide (PI) were added to each tube. These tubes were incubated for 10 minutes and protected from the light and finally, cell apoptosis was analyzed with the help of flow cytometry.

Gene Expression Study

Based on the outcome of the colony forming assay, FACS analysis and cellular mTOR enzyme assay, HB-UC-1 and HB-UC-5 were selected for the gene expression study. The culture medium composed of F12 Ham's, 5% FBS, 1% penicillin (100 U/mL) and 1% streptomycin (1 µg/ mL) were used to culture lung cancer cell line A549 in the CO₂ incubator at 37° C under 5% CO₂ and 95% relative humidity. The cells were seeded in the concentrations of 1×10⁶ cells per well in all the 6 well plates. After 24 hours of seeding, each compound viz. HB-UC-1 (0.06 µM, 0.03 µM), HB-UC-5 (0.22 µM, 0.11 µM) were added in two concentrations in duplicate. Among these two concentrations, one concentration corresponded to the IC₅₀ value of the compound found in the MTT assay and another concentration corresponded to the half of the IC₅₀. After 48 hours of incubation, media was removed from each well and washed with the 1X PBS buffer followed by the addition of 2 mL TRIzol[®] (Invitrogen). Treated and control cells were scrapped, transferred to the RNase free centrifuge tube and kept for 5 minutes at 37°C. Next, at 12,000 rpm, the centrifugation was carried out for 5 minutes at 4°C

and then the supernatants were transferred to the new centrifuge tubes followed by the addition of the 0.2 mL chloroform. . The resultant mixture were vortexed vigorously and kept at room temperature for 5 minutes. Again at 12000 RPM the centrifugation was performed for 15 minutes at 4°C. The upper aqueous phase from each sample was transferred to the new centrifuge tube. 500 µL ice-cold IPA was added to the aqueous phase and mixed gently followed by centrifugation at 4°C for 10-15 minutes. All the samples were kept on the ice. The supernatants were removed and the pellets were washed with 1mL 75% ethanol in DEPC treated water. The pellets were squirted in ethanol to dislodge from the bottom of the tube. Again at 7500 RPM the centrifugation was performed for 5 minutes at 4°C to isolate the RNA. The quantitative and qualitative analysis of the isolated RNA were carried out through NanoDrop 2000c (Thermo Scientific) and agarose gel electrophoresis, respectively. The RNA of each sample was converted to the cDNA using cDNA synthesis kit (Puregene Gentix). Resultant cDNA were utilized as a template to amplify the specific genes in the PCR reaction with gene specific forward and reverse pairs of primers i.e. E4BP4 (F5'GTCGACTGAATGACCTGGTTTT3'),(R5'TCTGGTAATCTTGAAAGTACACAGC3');eIF4EBP1 (F5'AGGAACCAGGATTATCTATGAC3'), (R5'TGTCCATCTCAAATTGTGACTC3'); PCK1(F5'AGGCAGTGAGGAAGTTCGTG3'),(R5'TACATGGTGCGGCCTTTCAT3') along with the housekeeping gene GAPDH. The amplicons were run on the 1.2% agarose gel using 1X TAE buffer and the image was taken with the help of Bio-Rad Gel Doc™. Further, the relative gene expressions were analyzed with the help of image J software and graphs were plotted using Microsoft Excel.

Western Blot Analysis

Lung cancer cell line (A549) was seeded into 6 well plates and allowed to grow in RPMI until 100% confluence. After confluence, the cells were treated overnight with starving RPMI. All the drug concentrations were dissolved in DMSO and serially diluted in starving RPMI to get desired drug concentration *i.e.* 0.1 to 5 µM of HB-UC-1 and HB-UC-5. After overnight starvation, media was replaced with drug solutions and treated for 3 hrs. After the treatment period, drug containing media was removed and washed twice with ice-cold PBS. The cells were lysed in lysis buffer containing protease inhibitor cocktail and the cell lysates were sonicated for protein

isolation. The protein content was quantified using Bradford's method (BioRad) and 10 μ M protein was subjected to gel electrophoresis with the aid of 10% SDS-polyacrylamide. Protein samples were transferred to nitrocellulose and immuno blotted against rabbit monoclonal antibodies; pAKT-s473.

Lifespan Animal Model

For the initial evaluation, a study was performed using the compounds HB-UC-1 and HB-UC-5 to evaluate the effect on the life span of the cancer-bearing animals. P₃₈₈D1 leukemia cells were procured from the NCCS, Pune, India and grown in the RPMI-1640 media supplemented with Fetal Bovine Serum (FBS) and penicillin-streptomycin solution. Female Balb/C mice were issued after the approval of protocol (IP/PCEM/PHD/22/2017/44) from the Institutional Animal Ethics Committee (IAEC) which is controlled by the Committee for the Purpose of Control and Supervision of Experiments on Animals (CPCSEA), Ministry of Social Justice and Empowerment, Government of India. Further, mice weighing between 30-42 gm were selected for the study and a proper day-night cycle was maintained. During the whole experiment, a proper condition of temperature ($23^{\circ}\text{C} \pm 2^{\circ}\text{C}$), humidity ($55 \pm 5\%$) was maintained. 1×10^5 cells per mice were injected intraperitoneally in all the mice (n=6) except control group on day 0 for the induction of cancer. The testing compounds viz. HB-UC-1 and HB-UC-5 dissolved in distilled water/PEG400 (1:1 ratio) were administered orally on day 0. The compounds HB-UC-1 and HB-UC-5 were given in the dose of 0.02 mg/kg along with Everolimus dissolved in the PEG400/deionized water in two phases. In the first phase, these compounds were given on day 1-3 and in the second phase they were given on day 7-9. On the other hand, control animal received only the vehicle during the experiment. This study was performed for the 30 days where throughout the experiment, deaths of animals were recorded. Percent survival of the animals was calculated with the help of the Kaplan-Meier curve. The selection of the dose was carried out based upon the previously reported literature of the standard drug. As our research focused on the mTOR inhibition and lung cancer treatment the dose of the compounds were selected based upon the reported mTOR inhibitor viz. Everolimus available for the treatment of lung cancer.

The standard drug Everolimus already checked at the dose of 2 mg/kg in the many lung cancer animal models. *In-vitro* biological evaluation of the compound HB-UC-1 on lung cancer cell line (A549) indicated that the compound HB-UC-1 ($\text{IC}_{50} = 0.06 \mu\text{M}$) was found to be 100 times more potent than the Everolimus ($\text{IC}_{50} = 6.09 \mu\text{M}$). In addition to this, the compound HB-UC-5 showed some

promising results in the specialized *In-Vitro* assay. Hence therefore the compounds HB-UC-1 and HB-UC-5 both were given in the dose of 0.02mg/kg. Detailed procedure and results are provided in supporting information.

Lung Cancer Animal Model

Induction of lung cancer was carried out with the help of Benzo[a] Pyrene procured from Sigma Aldrich. Benzo[a] Pyrene is one of the Polycyclic Aromatic Hydrocarbon (PAH) which is present in tobacco smoke and acts as a precursor of carcinogenic substance. It is the first carcinogen identified in cigarette smoke among the 60 established carcinogenic substances present in the tobacco smoke. Benzo[a] Pyrene produces highly carcinogenic substance in the presence of cytochrome P450-1A1 (CYP1A1) viz. Benzo[a] Pyrene-7,8-diol-9,10-epoxide (BPDE) which further resulted into the formation of free radical generation. This BPDE is usually responsible for forming the adduct with the DNA resulted into the mutation in the KRAS and TP53. This genetic mutation in the KRAS and TP53 ultimately resulted into the lung cancer. Another pathway which is responsible for the lung cancer involved the formation of the reactive oxygen species from the BPDE which ultimately resulted into a lung cancer. Female swiss-albino mice were chosen for the present research work. The weight of the animals was observed to be ranging from 15-30 gm and this was recorded immediately after their procurement. During the whole experiment, a proper condition of temperature ($23^{\circ}\text{C} \pm 2^{\circ}\text{C}$), humidity ($55 \pm 5\%$) and 12 hours light-dark cycle were maintained. All the animals were kept for a week in this condition so that they adapt to this condition. Standard pellet diet along with water was properly given to the animals *ad libitum*. All the methodology with the animals were followed after we got the approval of protocol (IP/PCEM/PHD/22/2017/43) from the Institutional Animal Ethics Committee (IAEC) which is controlled by the Committee for the Purpose of Control and Supervision of Experiments on Animals (CPCSEA), Ministry of Social Justice and Empowerment, Government of India. Detailed procedure and results are provided in supporting information.

Supporting Information

Details about Objectives of rational based drug design; Pharmacophore modelling and its validation; Virtual screening; Molecular docking studies and binding pose and hydrogen bond interactions; Details about spectral data of all synthetic THQ derivatives; FTIR, ^1H & ^{13}C NMR, Mass and HPLC Spectra of representative compounds along with X-Ray Crystallography of compound HB-UC-25 (CCDC number 1874590); Colony forming assay figure; Lifespan animal model figure; Lung cancer animal model and Histopathological analysis are given in the supporting information material file.

Note

All the animal experiments were performed in compliance with the relevant laws and institutional guidelines, and the experimental protocols carried out in present study were permitted by the Institutional Animal Ethics Committee (IAEC) of the Institute of Pharmacy, Nirma University, Ahmedabad, India, vide protocol numbers: IP/PCEM/PHD/22/2017/43 and IP/PCEM/PHD/22/2017/44. All the experimental methods are in line with CPCSEA guidelines, Ministry of Environment and Forests, Government of India.

Author Contributions

HB and UC conceptualized design, synthesis, and biological evaluation work. UC carried out wet-lab experimental works. UC performed flow cytometry analysis under guidance of RR. UC and BV concluded western blot studies. UC and AJ concluded *in-vivo* biological evaluation. HB and UC prepared manuscript for the publication.

Competing Financial Interests

There are no potential financial interests in the research work.

Acknowledgments

The authors HB/UC are highly thankful to Nirma University, Ahmedabad, India for providing necessary facilities to carry out the research work. UC is thankful to Department of Science and Technology (DST), Govt. of India for providing INSPIRE fellowship (IF140932).

References

1. Wood, S. L.; Pernemalm, M.; Crosbie, P. A.; Whetton, A. D. Molecular histology of lung cancer: From targets to treatments. *Cancer Treat. Rev.* **2015**, 41, 361-375.
2. Kan, Z.; Jaiswal, B. S.; Stinson, J.; Janakiraman, V.; Bhatt, D.; Stern, H. M.; Yue, P.; Haverty, P. M.; Bourgon, R.; Zheng, J.; Moorhead, M.; Chaudhuri, S.; Tomsho, L. P.; Peters, B. A.; Pujara, K.; Cordes, S.; Davis, D. P.; Carlton, V. E.; Yuan, W.; Li, L.; Wang, W.; Eigenbrot, C.; Kaminker, J. S.; Eberhard, D. A.; Waring, P.; Schuster, S. C.; Modrusan, Z.; Zhang, Z.; Stokoe, D.; de Sauvage, F. J.; Faham, M.; Seshagiri, S. Diverse somatic mutation patterns and pathway alterations in human cancers. *Nature*. **2010**, 466, 869-873.
3. Govindan, R.; Ding, L.; Griffith, M.; Subramanian, J.; Dees, N. D.; Kanchi, K. L.; Maher, C. A.; Fulton, R.; Fulton, L.; Wallis, J.; Chen, K.; Walker, J.; McDonald, S.; Bose, R.; Ornitz, D.; Xiong, D.; You, M.; Dooling, D. J.; Watson, M.; Mardis, E. R.; Wilson, R. K. Genomic Landscape of Non-Small Cell Lung Cancer in Smokers and Never-Smokers. *Cell*. **2012**, 150, 1121-1134.
4. Li, H.; Wang, S.; Takayama, K.; Harada, T.; Okamoto, I.; Iwama, E.; Fujii, A.; Ota, K.; Hidaka, N.; Kawano, Y.; Nakanishi, Y. Nicotine induces resistance to erlotinib via cross-talk between $\alpha 1$ nAChR and EGFR in the non-small cell lung cancer xenograft model. *Lung Cancer*. **2015**, 88, 1-8.
5. Santoro, I. L.; Ramos, R. P.; Franceschini, J.; Jamnik, S.; Fernandes, A. L. G. Non-small cell lung cancer in never smokers: a clinical entity to be identified. *Clinics*. **2011**, 66, 1873-1877.
6. Fumarola, C.; Bonelli, M. A.; Petronini, P. G.; Alfieri, R. R. Targeting PI3K/AKT/mTOR pathway in non small cell lung cancer. *Biochem. Pharmacol.* **2014**, 90, 197-207.
7. Asati, V.; Mahapatra, D. K.; Bharti, S. K. PI3K/AKT/mTOR and Ras/Raf/MEK/ERK signaling pathways inhibitors as anticancer agents: Structural and pharmacological perspectives. *Euro. J. Med. Chem.* **2016**, 109, 314-341.
8. Reddy, G. L.; Guru, S. K.; Srinivas, M.; Pathania, A. S.; Mahajan, P.; Nargotra, A.; Bhushan, S.; Vishwakarma, R. A.; Sawant, S. D. Synthesis of 5-substituted-1H-pyrazolo[4,3-d]pyrimidin-7(6H)-one analogs and their biological evaluation as anticancer agents: mTOR inhibitors. *Euro. J. Med. Chem.* **2014**, 80, 201-208.

9. Polivka, J.; Janku, F. Molecular targets for cancer therapy in the PI3K/AKT/mTOR pathway. *Pharmacol. Therapeut.* **2014**, 142, 164-175.
10. Zhang, Y. J.; Duan, Y.; Zheng, X. F. S. Targeting the mTOR kinase domain: the second generation of mTOR inhibitors. *Drug Discov. Today*. **2011**, 16, 325-331.
11. Jerusalem, G.; Rorive, A.; Collignon, J. Use of mTOR inhibitors in the treatment of breast cancer: an evaluation of factors that influence patient outcomes. *Breast Cancer*. **2014**, 6, 43-57.
12. Yang, H.; Rudge, D. G.; Koos, J. D.; Vaidialingam, B.; Yang, H. J.; Pavletich, N. P. mTOR kinase structure, mechanism and regulation. *Nature*. **2013**, 497, 217-223.
13. Chen, X.; Liu, M.; Tian, Y.; Li, J.; Qi, Y.; Zhao, D.; Wu, Z.; Huang, M.; Wong, C. C. L.; Wang, H. W.; Wang, J.; Yang, H.; Xu, Y. Cryo-EM structure of human mTOR complex 2. *Cell Res*. **2018**, 28, 518-528.
14. Chaube, U.; Chhatbar, D.; Bhatt, H. 3D-QSAR, molecular dynamics simulations and molecular docking studies of benzoxazepine moiety as mTOR inhibitor for the treatment of lung cancer. *Bioorg. Med. Chem. Lett.* **2016**, 26, 864-874.
15. Chaube, U.; Bhatt, H. 3D-QSAR, molecular dynamics simulations, and molecular docking studies on pyridoaminotropanes and tetrahydroquinazoline as mTOR inhibitors. *Mol. Divers.* 2017;21(3):741-759.
16. Bhatt H.; Patel P. Pharmacophore modeling, virtual screening and 3D-QSAR studies of 5-tetrahydroquinolinyldine aminoguanidine derivatives as sodium hydrogen exchanger inhibitors. *Bioorg. Med. Chem. Lett.* **2012**, 22, 3758-3765.
17. Patel S.; Patel B.; Bhatt H. 3D-QSAR studies on 5-hydroxy-6-oxo-1, 6-dihydropyrimidine-4-carboxamide derivatives as HIV-1 integrase inhibitors. *J. Taiwan Insti. Chem. Eng.* **2016**, 59, 61-68.
18. Patel, S.; Patel, B.; Pannecouque, C.; Bhatt, H. Design, synthesis and anti-HIV activity of novel quinoxaline derivatives. *Euro. J. Med. Chem.* **2016**, 117, 230-240.
19. Matthews, N.; Kitao, A.; Laycock, S.; Hayward, S. Haptic-Assisted Interactive Molecular Docking Incorporating Receptor Flexibility. *J. Chem. Inf. Model.* [Online early access]. DOI: 10.1021/acs.jcim.9b00112. Published Online: April 23, 2019.

20. Tighadouini, S.; Radi, S.; Abridach, F.; Benabbes, R.; Eddike, D.; Tillard, M. Novel β -Keto–Enol Pyrazolic Compounds as Potent Antifungal Agents. Design, Synthesis, Crystal Structure, DFT, Homology Modeling, and Docking Studies. *J. Chem. Inf. Model.* **2019**, *59*, 1398–1409.
21. Cordeiro, A.; Shaw, J.; O'Brien, J.; Blanco, F.; Rozas, I. Synthesis of 6-Nitro-1,2,3,4-tetrahydroquinoline: An Experimental and Theoretical Study of Regioselective Nitration. *Euro. J. Org. Chem.* **2011**, 2011, 1504-1513.
22. Mortensen, D. S.; Perrin-Ninkovic, S. M.; Shevlin, G.; Zhao, J.; Packard, G.; Bahmanyar, S.; Correa, M.; Elsner, J.; Harris, R.; Lee, B. G.; Papa, P.; Parnes, J. S.; Riggs, J. R.; Sapienza, J.; Tehrani, L.; Whitefield, B.; Apuy, J.; Bisonette, R. R.; Gamez, J. C.; Hickman, M.; Khambatta, G.; Leisten, J.; Peng, S. X.; Richardson, S. J.; Cathers, B. E.; Canan, S. S.; Moghaddam, M. F.; Raymon, H. K.; Worland, P.; Narla, R. K.; Fultz, K. E.; Sankar, S. Discovery of Mammalian Target of Rapamycin (mTOR) Kinase Inhibitor CC-223. *J. Med. Chem.* **2015**, *58*, 5323–5333.
23. Yu, T.; Li, N.; Wu, C.; Guan, A.; Li, Y.; Peng, Z.; He, M.; Li, J.; Gong, Z.; Huang, L.; Gao, B.; Hao, D.; Sun, J.; Pan, Y.; Shen, L.; Chan, C.; Lu, X.; Yuan, H.; Li, Y.; Li, J.; Chen, S. Discovery of Pyridopyrimidinones as Potent and Orally Active Dual Inhibitors of PI3K/mTOR. *ACS Med. Chem. Lett.* **2018**, *9*, 256–261.
24. Chaube, U.; Vyas, V.; Bhatt, H. Design and synthesis of potent N-phenylpyrimidine derivatives for the treatment of skin cancer. *RSC Advances*. **2016**, *6*, 10285-10297.
25. Kling, B.; Bücherl, D.; Palatzky, P.; Matysik, F. M.; Decker, M.; Wegener, J.; Heilmann, J. Flavonoids, Flavonoid Metabolites, and Phenolic Acids Inhibit Oxidative Stress in the Neuronal Cell Line HT-22 Monitored by ECIS and MTT Assay: A Comparative Study. *J. Nat. Prod.* **2014**, *77*, 446–454.
26. Kumar, V.; Chaudhary, A. K.; Dong, Y.; Zhong, H. A.; Mondal, G.; Lin, F.; Kumar, V.; Mahato, R. I. Design, Synthesis and Biological Evaluation of novel Hedgehog Inhibitors for treating Pancreatic Cancer. *Sci. Rep.* **2017**, *7*, 1665.
27. Li, Z.; Su, H.; Yu, W.; Li, X.; Cheng, H.; Liu, M.; Pang, X.; Zou, X. Design, synthesis and anticancer activities of novel otobain derivatives. *Org. Biomol. Chem.* **2016**, *14*, 277-287.

28. Han, T.; Li, J.; Xue, J.; Li, H.; Xu, F.; Cheng, K.; Li, D.; Li, Z.; Gao, M.; Hua, H. Scutellarin derivatives as apoptosis inducers: Design, synthesis and biological evaluation. *Euro. J. Med. Chem.* **2017**, 135, 270-281.
29. Farnaes, L.; Coufal, N.G.; Kauffman, C. A.; Rheingold, A. L.; Di Pasquale, A. G.; Jensen, P. R.; Fenical, W. Napyradiomycin Derivatives, produced by a Marine-Derived Actinomycete, Illustrate Cytotoxicity by Induction of Apoptosis. *J. Nat. Prod.* **2014**, 77, 15–21.
30. Khan, M.; Biswas, D.; Ghosh, M.; Mandloi, S.; Chakrabarti, S.; Chakrabarti, P. mTORC2 controls cancer cell survival by modulating gluconeogenesis. *Cell Death Discov.* **2015**, 1, 15016.
31. Yang, M.; Li, D.; Chang, Z.; Yang, Z.; Tian, Z.; Dong, Z. PDK1 orchestrates early NK cell development through induction of E4BP4 expression and maintenance of IL-15 responsiveness. *J. Exp. Med.* **2015**, 212, 253-265.
32. Zhan, M.; Deng, Y.; Zhao, L.; Yan, G.; Wang, F.; Tian, Y.; Zhang, L.; Jiang, H.; Chen, Y. Design, Synthesis, and Biological Evaluation of Dimorpholine Substituted Thienopyrimidines as Potential Class I PI3K/mTOR Dual Inhibitors. *J. Med. Chem.* **2017**, 60, 4023–4035.
33. Liu, J.; Liu, L.; Tian, Z.; Li, Y.; Shi, C.; Shi, J.; Wei, S.; Zhao, Y.; Zhang, C.; Bai, B.; Chen, Z.; Zhang, H. In Silico Discovery of a Small Molecule Suppressing Lung Carcinoma A549 Cells Proliferation and Inducing Autophagy via mTOR Pathway Inhibition. *Mol. Pharm.* **2018**, 15, 5427–5436.
34. Mohamed, K. O.; Zaki, I.; El-Deen, I. M.; Abdelhameid, M. K. A new class of diamide scaffold: Design, synthesis and biological evaluation as potent antimitotic agents, tubulin polymerization inhibition and apoptosis inducing activity studies. *Bioorg. Chem.* **2019**, 84, 399-409.
35. Lane, H. A.; Wood, J. M.; McSheehy, P. M.; Allegrini, P. R.; Boulay, A.; Brueggen, J.; Littlewood-Evans, A.; Maira, S. M.; Martiny-Baron, G.; Schnell, C. R.; Sini, P.; O'Reilly, T. mTOR Inhibitor RAD001 (Everolimus) Has Antiangiogenic/Vascular Properties Distinct from a VEGFR Tyrosine Kinase Inhibitor. *Clin. Cancer Res.* **2009**, 15, 1612-1622.

36. Bourderioux, A.; Naus, P.; Perlikova, P.; Pohl, R.; Pichova, I.; Votruba, I.; Dzubak, P.; Konecny, P.; Hajduch, M.; Stray, K. M.; Wang, T.; Ray, A. S.; Feng, J. Y.; Birkus, G.; Cihlar, T.; Hocek, M. Synthesis and Significant Cytostatic Activity of 7-Hetaryl-7-deazaadenosines. *J. Med. Chem.* **2011**, 54, 5498-5507.
37. Kasala, E. R.; Bodduluru, L. N.; Barua, C. C.; Gogoi, R. Antioxidant and antitumor efficacy of Luteolin, a dietary flavone on benzo(a)pyrene-induced experimental lung carcinogenesis. *Biomed. Pharmacother.* **2016**, 82, 568-577
38. Bodduluru, L. N.; Kasala, E. R.; Barua, C. C.; Karnam, K. C.; Dahiya, V.; Ellutla, M. Antiproliferative and antioxidant potential of hesperetin against benzo(a)pyrene-induced lung carcinogenesis in Swiss albino mice. *Chem. Biol. Interact.* **2015**, 242, 345-352.
39. Selvendiran, K.; Banu, S. M.; Sakthisekaran, D. Protective effect of piperine on benzo(a)pyrene-induced lung carcinogenesis in Swiss albino mice. *Clin. Chim. Acta.* **2004**, 350, 73-78.

Figure Captions

Figure 1. (A) Docking interactions of standard co-crystallized ligand PI-103 with the mTOR protein (4JT6) (B) Docking pose of compound AZD-2014 with the mTOR protein (C) pharmacophore based virtual screening gave Tetrahydroquinoline as a core scaffold while required substitutions identified through the knowledge based drug designing approach using AZD-2014 as a standard molecule and (D) 3D-QSAR approach.

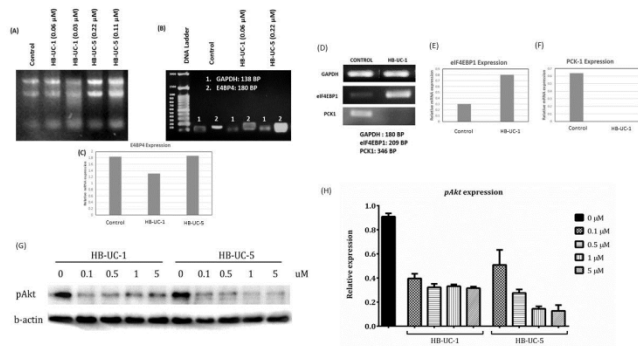
Figure 2. Synthetic Scheme and Procedure: Reagents and conditions: (i) Triethylamine, DCM, Stirring for 24 hr. (ii) $\text{KNO}_3/\text{H}_2\text{SO}_4$, DCM, stirring at 0 to RT for 2 hr. (iii) Pyrrolidine, DCM, stirring for 5 min. (iv) Triethylamine, DCM, Stirring for 24 hr. (v) $\text{Zn}/\text{NH}_4\text{Cl}$, Methanol, Heating at 60°C for 6 hr. (vi) Triethylamine, DCM, Stirring for 1 to 2 hr.

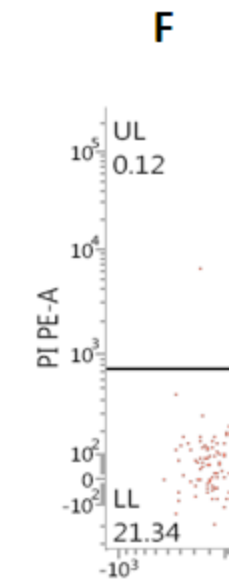
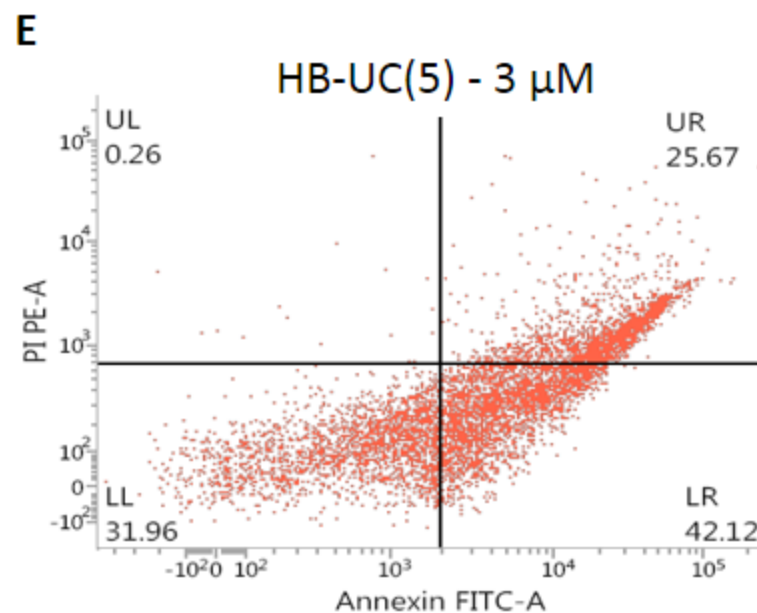
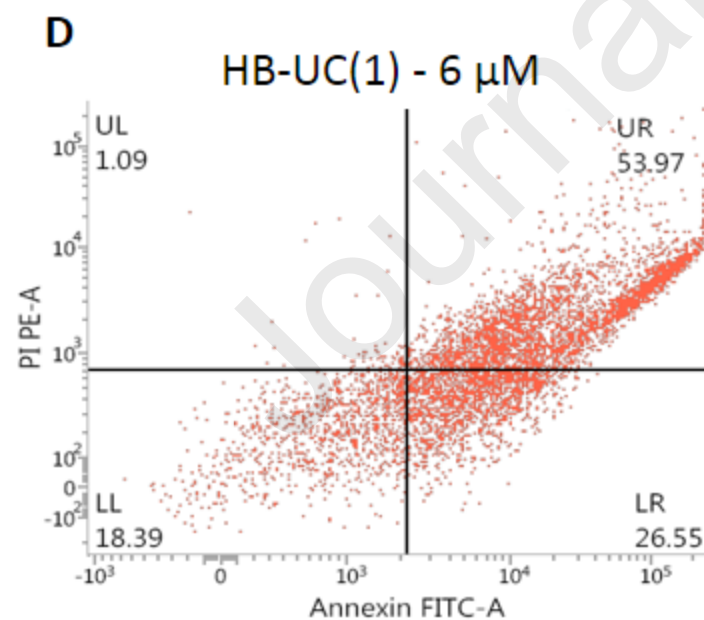
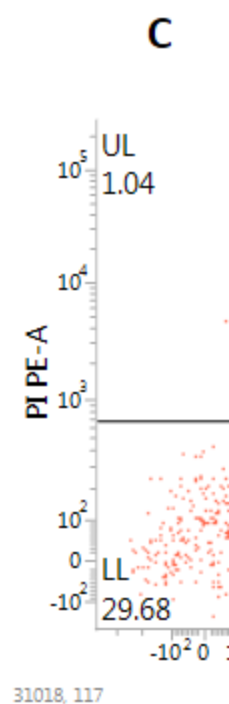
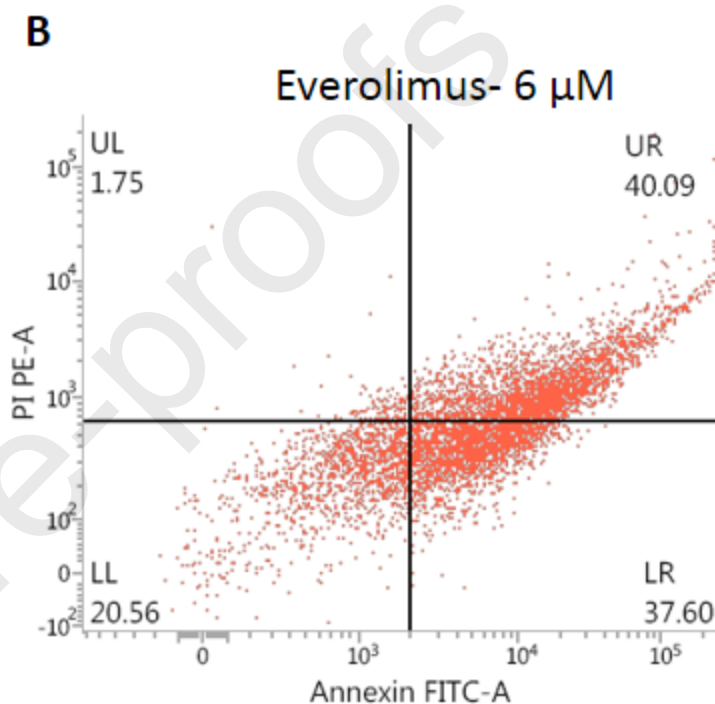
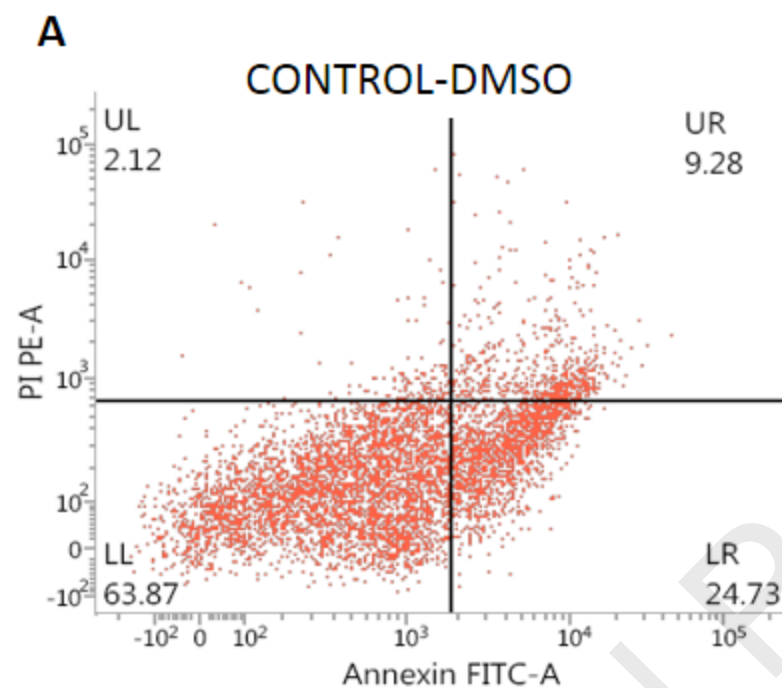
Figure 3. (A) DMSO control cells of lung cancer (A549); (B) Effect of Everolimus at $6\ \mu\text{M}$ on apoptosis (C) Effect of compound HB-UC-1 at $3\ \mu\text{M}$ (D) and at $6\ \mu\text{M}$ on apoptosis (E) Effect of compound HB-UC-5 at $3\ \mu\text{M}$ (F) and $6\ \mu\text{M}$ on apoptosis.

Figure 4. (A) Isolated mRNA from control and treatment groups from A549 lung cancer cell line (B) Effect of compound HB-UC-1 and HB-UC-5 compared to the control group on the E4BP4 gene expression (C) E4BP4 gene expression reduced due to the effect of compound HB-UC-1 which were analyzed by image J software and graph was plotted. (D) Effect of compound HB-UC-1 ($0.06\ \mu\text{M}$) on the downstream regulators of mTORC1 (eIF4EBP1) and mTORC2 (PCK1) (E) All the expressions were analyzed by image J software and graph was plotted where expression of eIF4EBP1 is increased and (F) expression of PCK1 decreased. (G) Lung Cancer (A549) cell line treated with compound HB-UC-1 and HB-UC-5 at indicated concentration and further western blot analysis was done in the cell lysate with the aid of pAKT antibody. Immunoblotting revealed the inhibitory activity of compound HB-UC-1 and HB-UC-5 on

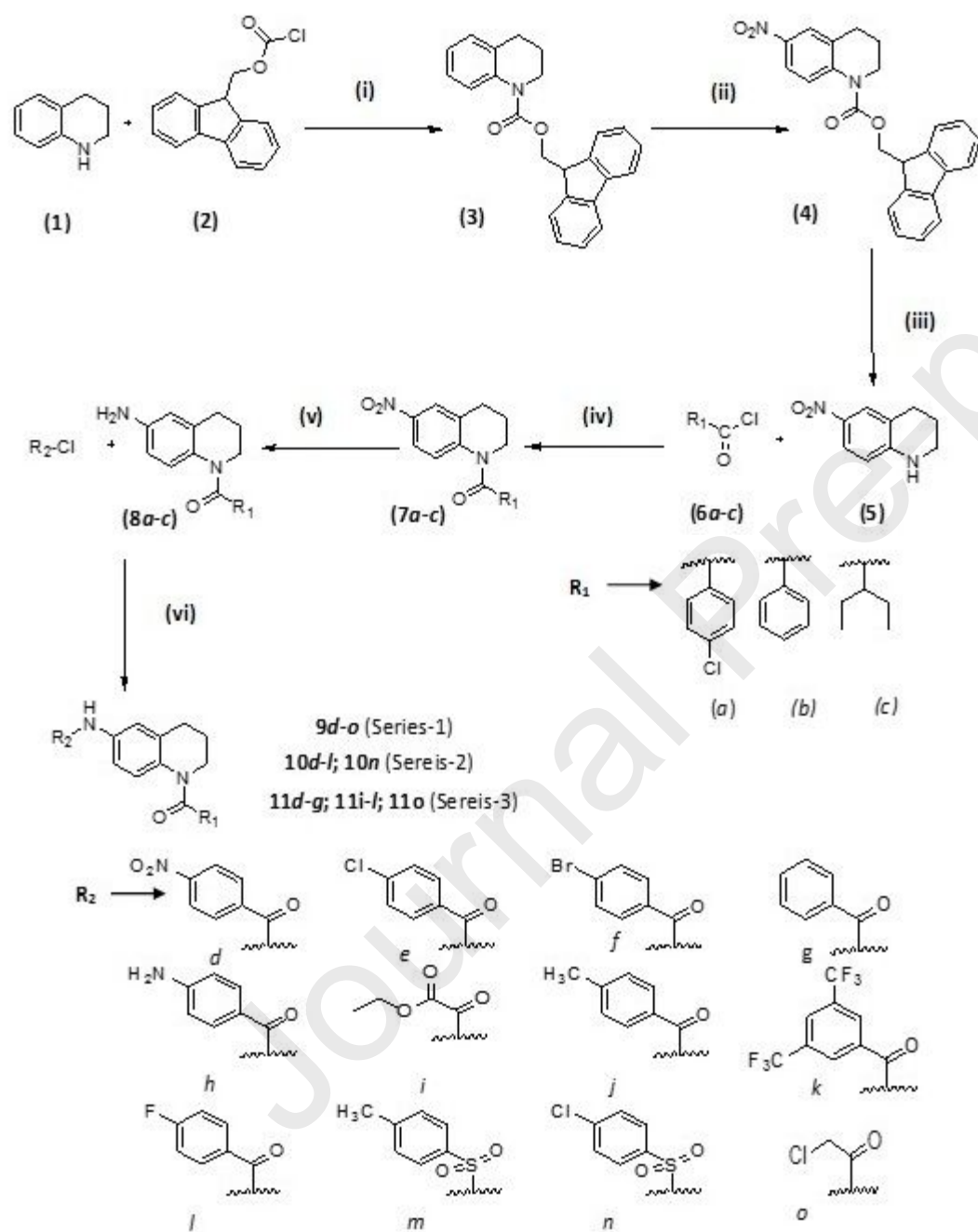
mTORC2 as these compounds hindered the phosphorylation of AKT S473. (H) Further quantification was done with the help of image J software and statistical analysis was carried out with the help of Graph pad prism.

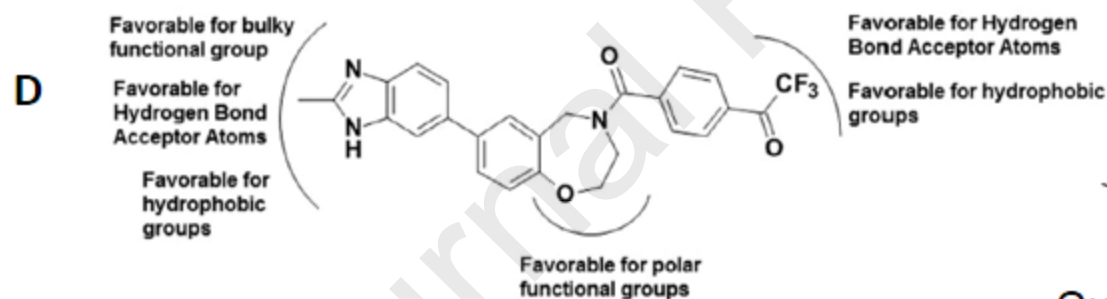
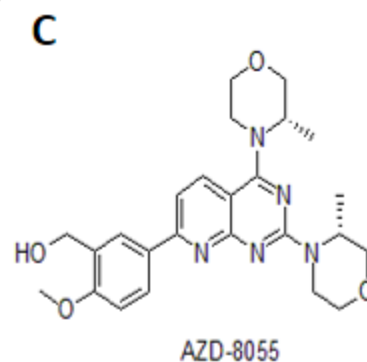
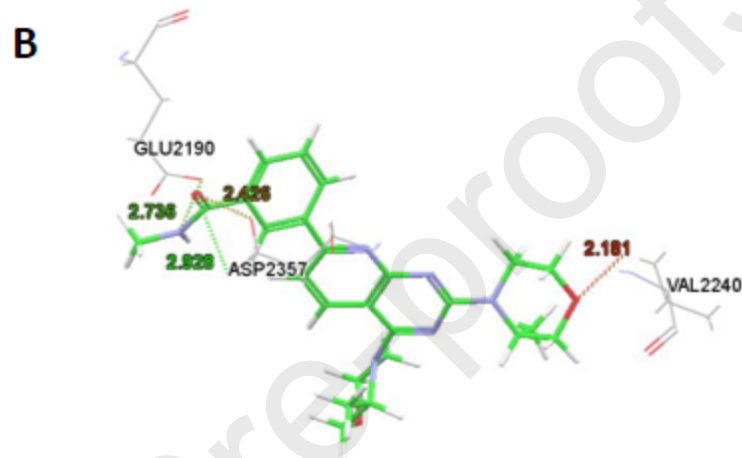
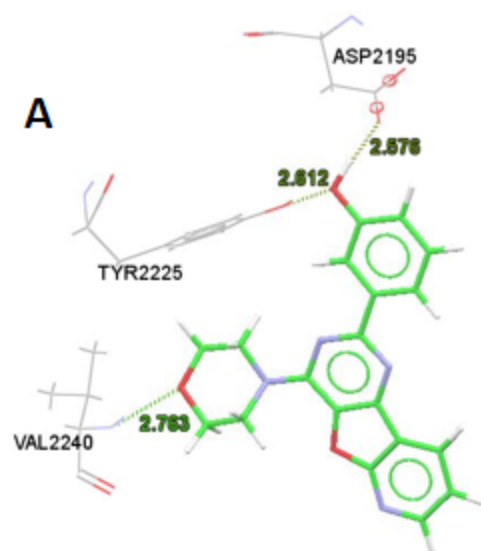
Figure 5. Measurement of (A) LDH (B) GGT (C) MDA (D) GSH and (E) Catalase after treatment with Everolimus (Eve) along with the compounds HB-UC-1 and HB-UC-5 where each bar represents mean \pm SEM, n=6 animals, (Oneway ANOVA followed by Dunnett's multiple comparison test), * = $p < 0.05$ vs. Disease Control Group (DC). (F) Lung photographs of Diseased Control (DC), Normal Control (NC) and treatment groups (Everolimus, HB-UC-1 and HB-UC-5) (G) Histopathological sections observed with the help of H & E staining revealed the different features of lung tissue from the Diseased Control (DC), Normal Control (NC) and treatment groups (Everolimus, HB-UC-1 and HB-UC-5).





31018, 117

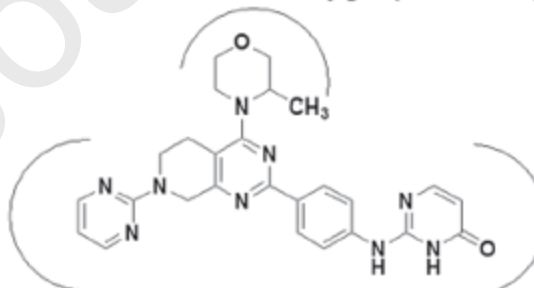




Favorable for polar functional groups

Bulky groups favored region

Favored for bulky groups, proton acceptor atoms, polar functional groups



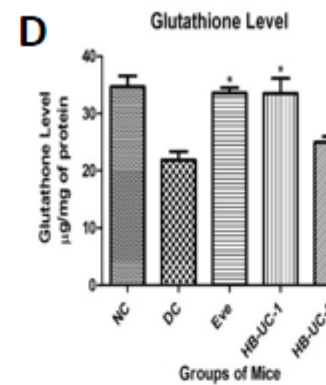
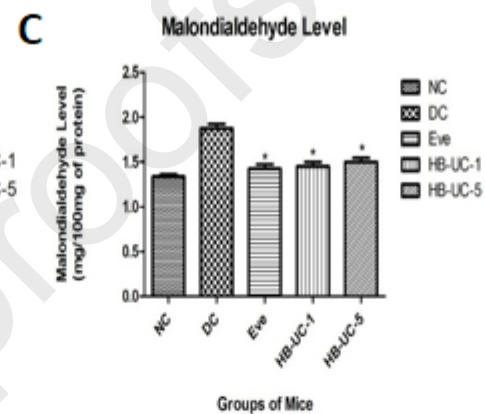
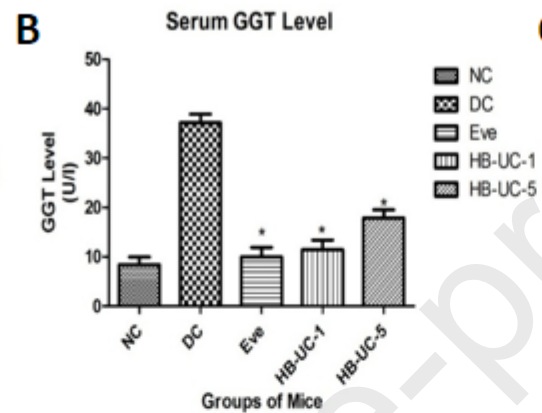
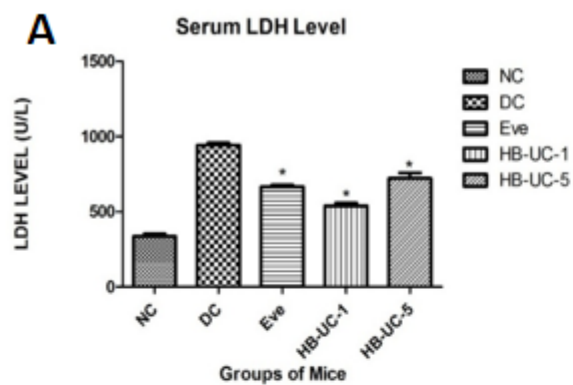
Favored for combination of electropositive and electronegative groups in the ring, proton donor atoms, polar functional groups

Outcome of 3D-QSAR

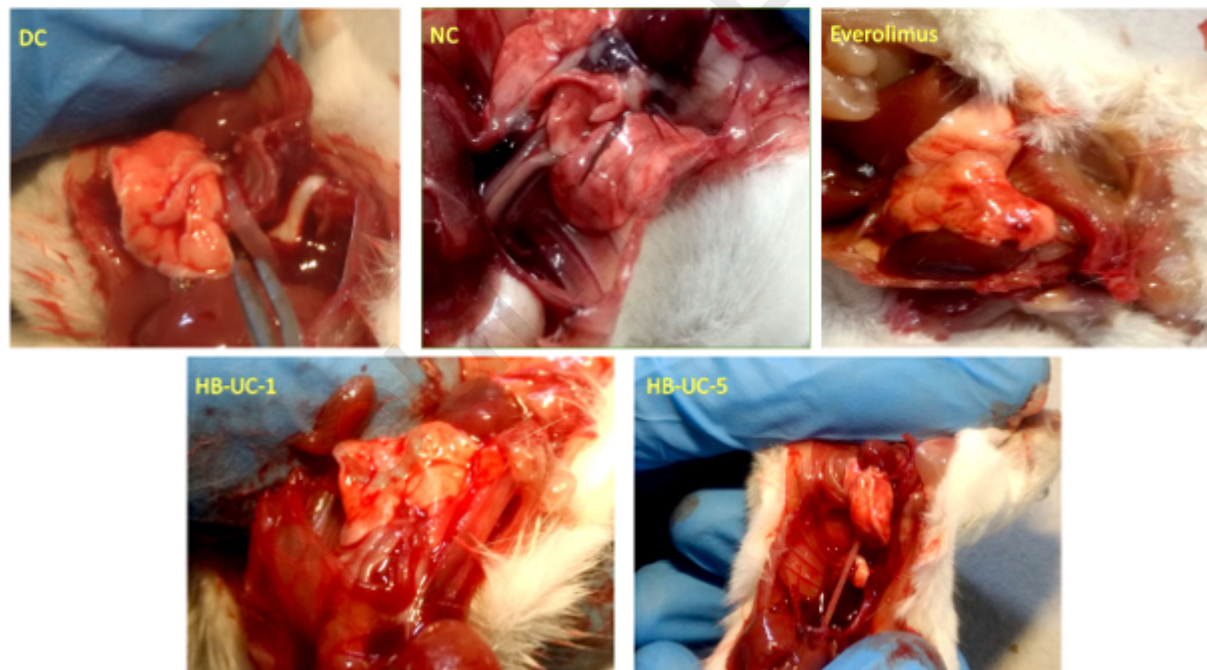
Incorporation of H-bond responsible for the bond with the of the

Amide bond incorporated for the improvement of the water solubility and less residence time in heptocyte

Pharmacophore based vi



F



G

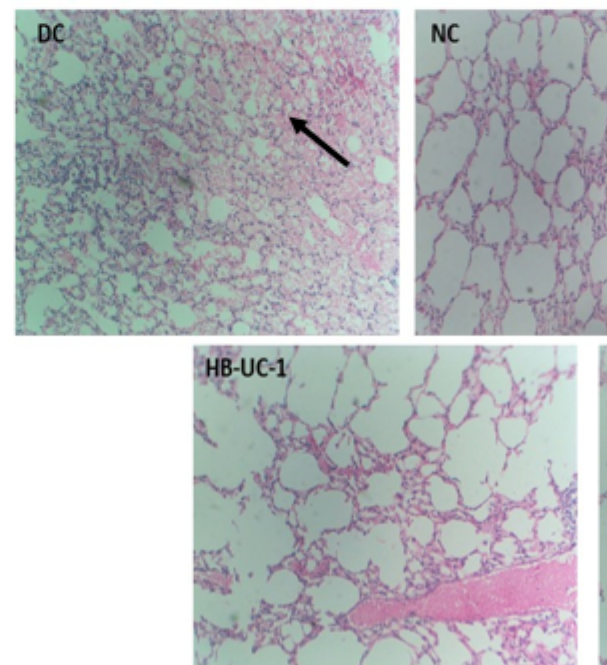
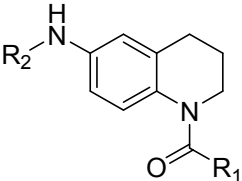
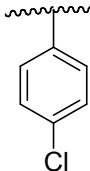
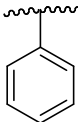
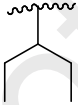
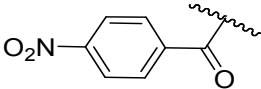
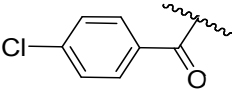
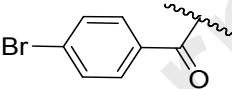
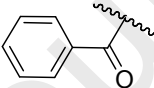
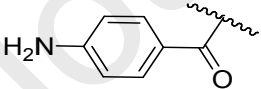
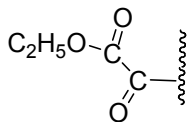
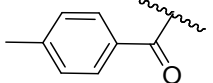
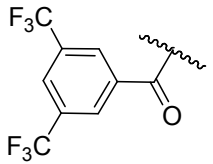
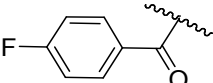
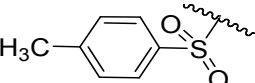
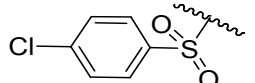
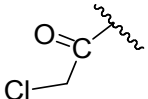
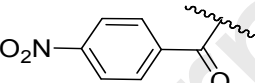
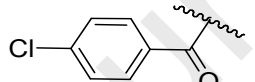
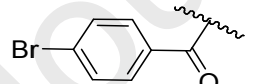
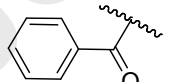
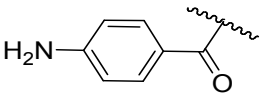
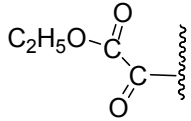
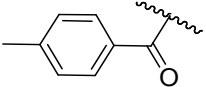
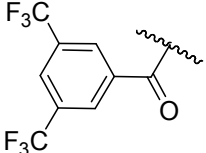
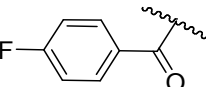
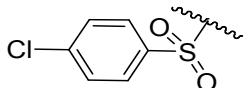
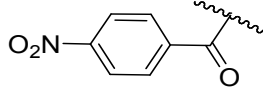
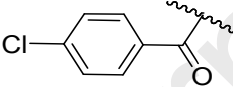
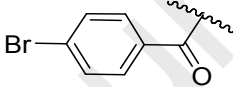
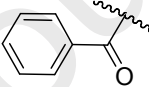
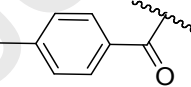
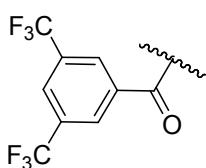
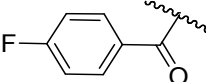
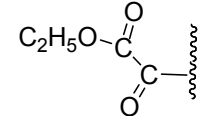
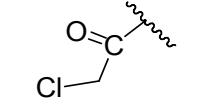


Table 1. *In vitro* antiproliferative activity of synthesized compounds on A-549, AGS, HCT-15, B16F1 and VERO cell lines and cellular mTOR enzyme activity.

<div style="display: flex; align-items: center; justify-content: center;"> <div style="text-align: center;">  </div> <div style="margin: 0 20px;">R₁ =</div> <div style="display: flex; gap: 20px;"> <div style="text-align: center;">  Series-I </div> <div style="text-align: center;">  Series-II </div> <div style="text-align: center;">  Series-III </div> </div> </div>							
Compounds	Substitution (R ₂)	AGS IC ₅₀ (μM)	A-549 IC ₅₀ (μM)	HCT-15 IC ₅₀ (μM)	B16F1 IC ₅₀ (μM)	VERO IC ₅₀ (μM)	Cellular mTOR activity in IC ₅₀ (μM)
Everolimus	-	9.69± 0.29	6.09±0.21	0.69±0.34	9.99±0.37	>25	7.5±0.21
Cisplatin	-	6.81±0.27	3.15±0.19	>25	>25	14.66±0.32	-
AZD-8055	-	5.73±0.54	8.17±0.25	0.95±0.54	>25	>25	1.5±0.31
PI-103	-	1.46±0.22	1.65±0.34	9.10±0.79	21.23±0.27	>25	-
Series-I							
HB-UC-1		16.35±0.21	0.06±0.27	>25	>25	>25	3.17±0.19
HB-UC-2		>25	>25	>25	>25	>25	11.06±0.34
HB-UC-3		>25	0.657±0.39	>25	>25	>25	4.77±0.18
HB-UC-4		>25	0.971±0.16	>25	24.18±0.14	>25	13.09±0.23
HB-UC-5		>25	0.224±0.45	>25	>25	>25	3.42±0.34

HB-UC-6		>25	0.158±0.38	>25	>25	>25	4.02±0.48
HB-UC-7		>25	3.730±0.54	>25	>25	>25	15.75±0.51
HB-UC-9		>25	3.280±0.39	>25	>25	>25	18.24±0.45
HB-UC-10		23.06±0.21	7.820±0.45	>25	>25	>25	14.74±0.38
HB-UC-11		>25	>25	>25	>25	>25	>25
HB-UC-13		>25	>25	>25	>25	>25	>25
HB-UC-14		>25	>25	7.37±0.64	3.16±0.21	>25	>25
Series-II							
HB-UC-15		>25	>25	11.08±0.08	>25	>25	>25
HB-UC-16		>25	>25	>25	>25	>25	>25
HB-UC-17		>25	>25	>25	>25	>25	>25
HB-UC-18		>25	>25	>25	>25	>25	>25

HB-UC-19		>25	>25	>25	>25	15.43±0.41	>25
HB-UC-20		>25	>25	>25	>25	>25	>25
HB-UC-21		>25	>25	>25	>25	>25	>25
HB-UC-23		>25	>25	>25	>25	>25	>25
HB-UC-24		>25	>25	>25	>25	3.38±0.31	>25
HB-UC-25		>25	>25	>25	>25	>25	>25
Series-III							
HB-UC-31		>25	>25	10.04±0.13	>25	>25	>25
HB-UC-32		>25	>25	>25	>25	2.04±0.32	>25
HB-UC-33		>25	17.36±0.15	>25	17.41±0.23	>25	>25
HB-UC-34		>25	>25	>25	>25	>25	>25
HB-UC-36		>25	>25	9.63±0.31	>25	>25	>25

HB-UC-37		>25	25±	12.24±0.12	>25	>25	>25
HB-UC-38		>25	22.9±0.21	>25	>25	>25	>25
HB-UC-39		>25	>25	>25	>25	2.46±0.15	>25
HB-UC-41		>25	16.24±0.12	>25	>25	>25	>25

Results are mean of three determination and are given as ±SEM

Table 2. Effect of the compounds HB-UC-1 and HB-UC-5 on the lifespan of the animals along with their survival time after the induction of the leukemia.

Groups	Percentage (%) Animal Survived (On 30 th Day)	Mean Survival Time (MST)
Normal Control (NC)	100	22.5 Days
Disease Control (DC)	0	15 Days
HB-UC-1	83	22.5 Days
HB-UC-5	16	22.5 Days

Table 3. Effect of Everolimus, HB-UC-1 and HB-UC-5 on body weight and lung weight.

Parameters	Group-1 Normal Control	Group-2 Disease Control	Group-3 Everolimus	Group-4 HB-UC-1	Group-5 HB-UC-5
Number of mice	6	6	6	6	6
Body Weight (gm)	23.50 ± 0.42	16.33 ± 0.61	23.50 ± 0.76	22.33 ± 0.33	20.33 ± 0.33
Weight of Lung (mg)	137.66±6.54	236.50±5.15	139.25±1.43	149.50±6.48	167.16±4.88

Each column represents mean ± SEM, n = 6 mice (Oneway ANOVA followed by Dunnett's multiple comparison test)



Highlights

- Novel tetrahydroquinoline derivatives were designed by SBDD and LBDD approach
- Novel derivatives were synthesized and confirmed by the spectral & XRD analysis
- All derivatives were screened *in-vitro* against various cell line & mTOR enzyme
- FACS analysis, gene expression study & western blot analysis supported study
- Potent leads were evaluated by life span and bezopyrene lung cancer animal model

Declaration of interests

☒ The authors declare that they have no known competing financial interests or personal relationships that could have appeared to influence the work reported in this paper.

☐ The authors declare the following financial interests/personal relationships which may be considered as potential competing interests:

--